

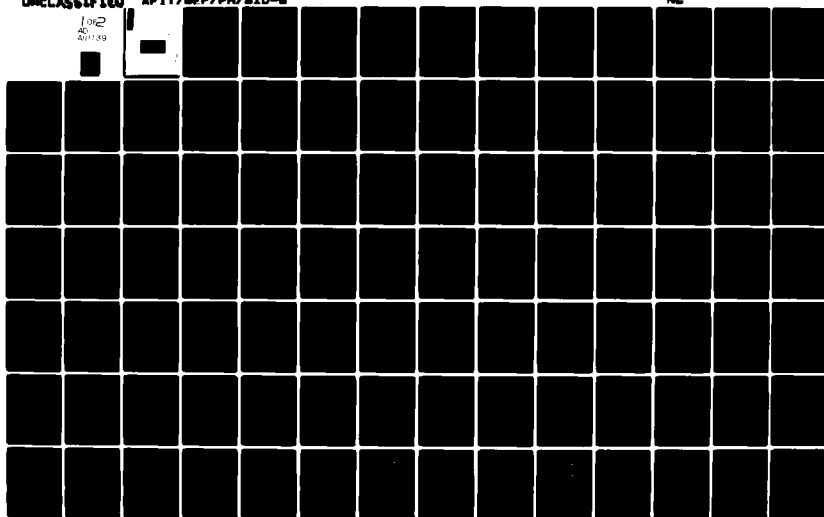
AD-A111 139

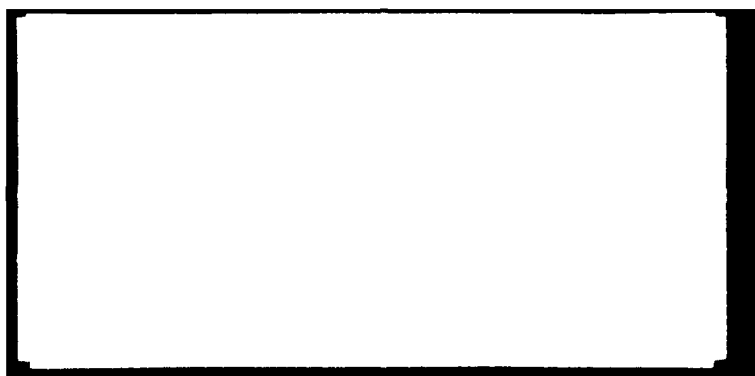
AIR FORCE INST OF TECH WRIGHT-PATTERSON AFB OH SCHOO--ETC F/G 20/2  
DEPTH-RESOLVED LUMINESCENCE OF GALLIUM ARSENIDE USING ION ETCHING--ETC(U)  
DEC 81 H T MACLIN  
AFIT/SEP/PH/SID-6

UNCLASSIFIED

ML

1002  
20  
20109





AFIT/GEP/PH/81D-6

LEVEL

II

①

DEPTH-RESOLVED LUMINESCENCE  
OF GALLIUM ARSENIDE USING  
ION ETCHING  
THESIS

AFIT/GEP/PH/81D-6

Myron T. Maclin  
Captain USAF

Approved for public release; distribution unlimited.

DEPTH-RESOLVED LUMINESCENCE  
OF GALLIUM ARSENIDE USING  
ION ETCHING

THESIS

Presented to the Faculty of the School of Engineering  
of the Air Force Institute of Technology  
Air Training Command  
in Partial Fulfillment of the  
Requirements for the Degree of  
Master of Science

by

Myron T. Maclin

Captain USAF

Graduating Engineering Physics

December 1981

Accession For	
NTIS GRA&I	<input checked="" type="checkbox"/>
DTIC TAB	<input type="checkbox"/>
Unannounced	<input type="checkbox"/>
Justification	<input type="checkbox"/>
By	
Distribution	
Availability	
Dist	
A	

Approved for public release; distribution unlimited.

## Preface

The completion of this thesis project was a very beneficial educational experience which would not have been possible without the advice and assistance of others. I would like to express my thanks to my faculty advisor, Dr. Robert L. Hengehold, for the direction he provided throughout this project. I would like to thank the personnel of the AF Avionics Laboratory (AFWAL/AADR) and Capt. Manuel Key for providing the samples used in this study. The Avionics Lab personnel also provided their Dektak surface measuring device and quantities of liquid helium for which I am thankful. I would also like to express my gratitude for the fine technical assistance given to me by Jim Miskimen, George Gergal, and Ron Gabriel of the AFIT Physics Laboratory Staff. Mr. Jack Capehart and his associates in the Analog-Hybrid section of the ASD computer centers were very helpful in transferring the data on 101 paper tapes to computer cards. I would also like to thank Dr. T. W. Haas of the AF Materials Laboratory for his helpful discussions of ion etching techniques. Finally, I would like to thank my wife, Vicki, and children, Teresa and Billy, for their understanding during the time that I was absorbed in this project and for Vicki's help in typing the grading copy of this thesis.

## Contents

	<u>Page</u>
Preface . . . . .	ii
List of Figures . . . . .	v
List of Tables . . . . .	vii
Abstract . . . . .	viii
I. Introduction . . . . .	1
II. Theory . . . . .	4
Luminescence . . . . .	4
Simple Centers . . . . .	6
Complex Centers . . . . .	12
Electron Penetration Depths . . . . .	17
Laser Beam Penetration . . . . .	19
Ion Implantation . . . . .	20
Ion Etching . . . . .	22
III. Experiment . . . . .	28
The System . . . . .	28
Vacuum System . . . . .	30
Sample Holder . . . . .	33
Ion Bombardment . . . . .	33
Electron gun . . . . .	34
Laser . . . . .	35
Beam Detectors . . . . .	35
Optics . . . . .	37
Spectrometer . . . . .	39
Photomultiplier . . . . .	39

Amplifiers and Discriminator . . . . .	41
Multichannel Analyzer . . . . .	41
Procedures . . . . .	42
Chamber Evacuation . . . . .	42
Sample Cooling . . . . .	43
Ion Beam Alignment . . . . .	45
Ion Etching . . . . .	46
Electron Beam Alignment . . . . .	48
Spectrometer Alignment . . . . .	49
Optics Alignment . . . . .	50
Luminescence Measurements . . . . .	50
IV. Results and Discussion . . . . .	53
Ion Gun Performance . . . . .	56
Luminescence in Virgin GaAs . . . . .	61
Luminescence in Implanted, Annealed GaAs . .	65
Luminescence in Annealed GaAs . . . . .	72
Luminescence in Implanted, Unannealed GaAs .	72
Luminescence in Heavily Implanted GaAs . . .	76
V. Conclusions and Recommendations . . . . .	83
Conclusions . . . . .	83
Recommendations . . . . .	85
Bibliography . . . . .	87
Vita . . . . .	90

## List of Figures

<u>Figure</u>		<u>Page</u>
1	Simple Energy Band Diagram . . . . .	5
2	Pertrubed Energy Band Diagram . . . . .	15
3	Theoretical Ion Implantation Range Distribution . . . . .	23
4	Dependence of Etch Rate on Ion Energy and Ion Current Density . . . . .	25
5	Luminescence Measuring System Schematic . . . . .	29
6	Vacuum Chamber, Top View . . . . .	31
7	Ion Detector . . . . .	37
8	Optics Arrangement . . . . .	39
9	Luminescence From Surface of Sample 4, Various Excitation Sources . . .	62
10	Cathodoluminescence From Sample 4 at Various Etch Depths. . . . .	63
11	Photoluminescence of Sample 6 at Various Etch Depths . . . . .	67
12	Photo- and Cathodoluminescence from Surface of Sample 6 . . . . .	69
13	Cathodoluminescence of Sample 6 at Various Etch Depths . . . . .	70
14	Cathodoluminescence of Surface of Sample 8 . . . . .	73

15	Cathodoluminescence of Sample 7 at Various Etch Depths . . . . .	75
16	Photoluminescence from Surface of Samples 6 and 9 . . . . .	77
17	Cathodoluminescence from Surface of Samples 6 and 9 . . . . .	79
18	Cathodoluminescence of Sample 9 at Various Beam Currents . . . . .	81
19	Cathodoluminescence of Sample 9 at Various Temperatures . . . . .	82

## List of Tables

Table		Page
I	Sample Summary	55
II	Variation of Ion Current with Beam Energy. . . . .	57
III	Measured Etch Depths for Selected Samples . . . . .	59

### Abstract

A system was assembled for obtaining depth-resolved, low-temperature luminescence data from GaAs using ion etching. This system was tested on virgin and silicon implanted, liquid-encapsulated Czochralski (LEC) grown GaAs. It was found to be effective in detecting lattice damage in annealed and unannealed Si-implanted GaAs. Cathodoluminescence, using a low-voltage (900-1500 V), high current (50-100  $\mu$ A) electron gun, was found to be extremely sensitive to surface defects. Very intense, broad ( $\sim$ 80 meV) luminescence bands were observed near 1.44 eV in GaAs implanted with  $10^{14}$  Si ions/cm<sup>2</sup> and near 1.35 eV in GaAs implanted with  $10^{15}$  Si ions/cm<sup>2</sup>. The center(s) responsible for this luminescence was confined to a surface layer 500-1000 Å thick.

DEPTH-RESOLVED LUMINESCENCE  
OF GALLIUM ARSENIDE USING  
ION ETCHING

I. Introduction

The United States Air Force has a growing need for high-speed semiconductor devices that can operate in the high-temperature environments found in many Air Force Systems. With proper addition of impurities (doping), the semiconductor gallium arsenide (GaAs), has many of the electrical properties required for such devices.

Gallium arsenide is an intermetallic compound formed from a group III element (gallium) and a group V element (arsenic) which crystallizes in the zincblende crystal structure. It has physical properties similar to the group IV semiconductors silicon and germanium but the slightly ionic bonding in GaAs results in a material with higher electron mobility. High electron mobility makes possible the development of high-speed electronic devices. Additionally, the combination of these two elements results in a crystalline material with a wider band gap energy than is found in silicon or germanium. This wider band gap makes possible devices that operate reliably at higher temperatures than devices made of silicon or germanium.

These properties make GaAs a very attractive semiconductor in view of the Air Force requirements stated above.

Pure GaAs is highly resistive and must be doped for many applications. One method of doping semiconductors which allows accurate three-dimensional control of dopant concentrations is ion implantation. The ion implantation process requires that impurity atoms be ionized, accelerated to high energies, and allowed to bombard the target crystal. One of the inherent disadvantages of ion implantation is that it causes a tremendous amount of lattice disorder in the implant layer of the crystal. Much of this disorder is repaired and the impurities are activated by annealing the substrate. However, some disorder remains and this disorder affects the optical and electrical properties of the crystal. If GaAs is to be developed to its fullest potential, we must understand the nature and the effects of these lattice disorders.

One analysis method which is particularly sensitive to lattice disorder or defects in semiconductors is luminescence. Luminescence is the process in which a portion of the energy absorbed by a material is emitted in the form of electromagnetic radiation. If the excitation energy is provided by a beam of energetic electrons, the emission is called cathodoluminescence. If the excitation energy is transmitted optically, the luminescence is called

photoluminescence. The luminescence spectra from GaAs is affected by the type and quantity of both impurities and lattice defects present in the sample. By exciting luminescence from a thin layer of the surface, then removing that surface layer and exciting the next layer, and repeating this cycle several times, one can obtain depth-resolved luminescence data. This data should reflect the concentrations of various types of impurities and lattice defects as a function of depth into the crystal.

The purpose of this study was to establish techniques for ion etching and luminescence excitation and measurements which could be used to study damaged surfaces, and further, to test these techniques on selected GaAs samples. Ion etching was accomplished with a commercially available ion bombardment gun and luminescence was excited in the samples with low energy electron beams and with a 15 mW He-Ne laser. The techniques were demonstrated on samples of bulk GaAs grown by the Liquid-Encapsulated Czochralski (LEC) method. Both undoped and silicon implanted samples were studied.

The theory relevant to this thesis is presented in chapter II. A description of the experimental apparatus and the procedures used is presented in chapter III. The experimental results obtained are discussed in chapter IV, and some conclusions and recommendations are presented in the final chapter.

## II. Theory

In this chapter, that theory which is necessary for an adequate understanding of the discussion of results and of the conclusions reached will be presented. The major topics appearing in this section are: luminescence, electron beam and laser penetration, ion implantation and ion etching.

### Luminescence

When a material absorbs energy, part of the absorbed energy heats the material and part of it is re-radiated. Crystalline solids such as GaAs emit radiation which is characteristic of the various allowed energy levels within the crystal. This radiation is referred to as luminescence. It is the result of radiative recombinations of electron-hole pairs produced by the absorbed energy. This luminescence results from the return of electron-hole pairs to their ground energy level after being raised to one of many excited states by the absorbed energy. The literature is full of reports of many different luminescence lines in GaAs. Some of these emission lines can be explained using the simple model of crystal energy levels illustrated in Figure 1. The radiative processes depicted in Figure 1 are said to result from simple recombination centers.

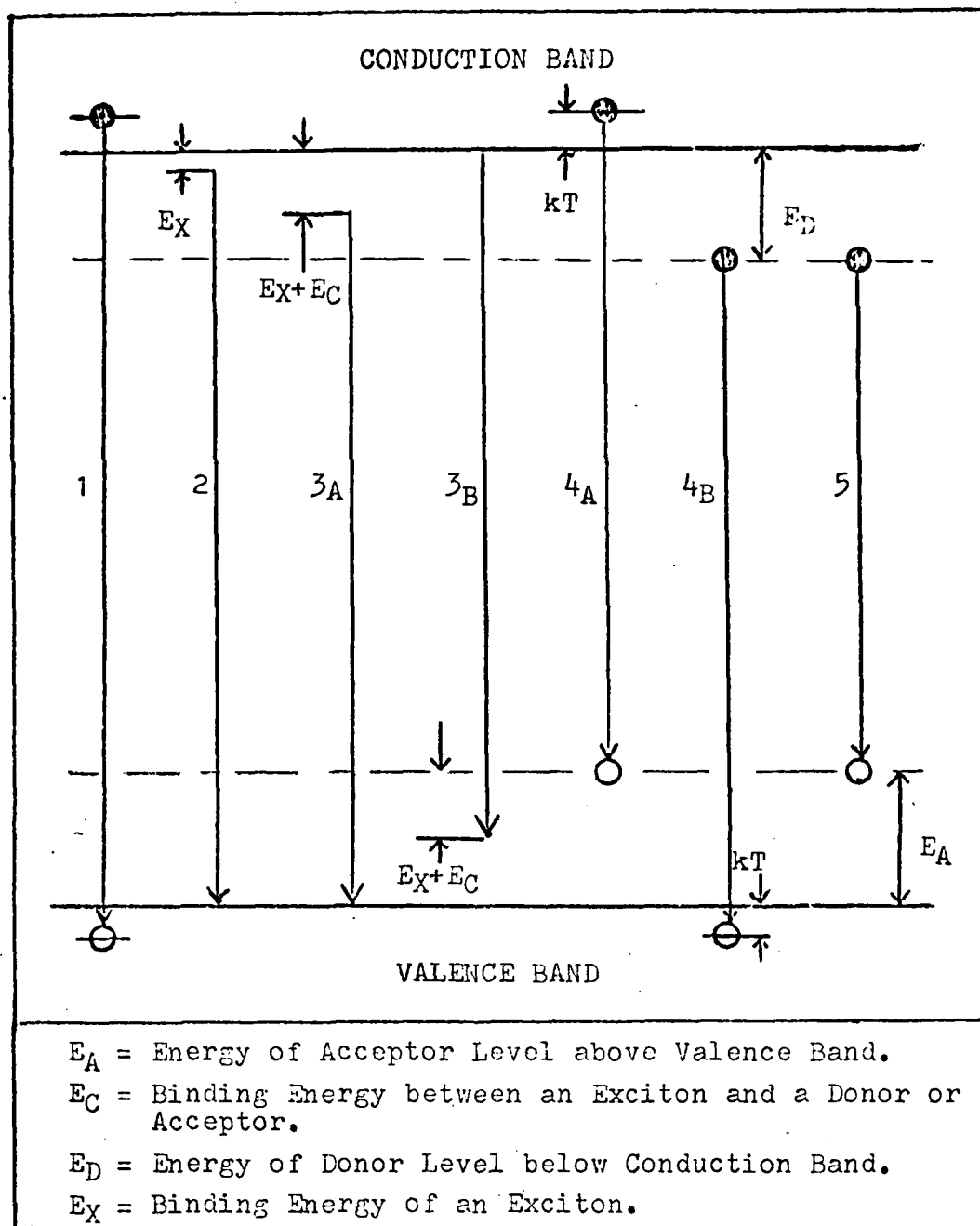


Fig. 1. Simple Energy Band Diagram

These simple centers account for much of the most commonly observed spectra from GaAs. However, many luminescence peaks have been observed that cannot, because of their energy level and/or line width, be explained by this simple model. These peaks are generally attributed to radiative complexes. A complex is a radiative center that does not fit the model of Figure 1. Complexes are believed to result from the interaction of impurities and/or crystal defects which cause localized perturbations in the allowed energy levels and, in some cases, act as pseudo-molecules with their own set of excited energy states (Ref. 29:1663).

#### Simple Centers

The radiative recombinations depicted in Figure 1 are all due to simple center recombinations. Simple center recombinations include: free electron-free hole recombinations, exciton annihilation, free electron-bound hole and bound electron-free hole recombinations, and bound electron-bound hole recombinations.

Line 1 in Figure 1 represents a free electron-free hole recombination. The photon emitted from this recombination would have energy:

$$E = E_G + 2 kT \quad (1)$$

where

$E$  = the energy of the emitted photon

$E_G$  = the energy of the forbidden gap between  
the valence and conduction bands, 1.521 eV  
in GaAs at 21° K, (Ref. 26)

$k$  = Boltzmann's constant,  $8.61708 \times 10^{-5}$  eV/°K

$T$  = temperature in degrees Kelvin

At low temperature, this energy is very close to  $E_G$  since, for example, at liquid helium temperature, 4.2° K,  $kT = 0.3619$  milli-electron volts (meV). Observations of the free electron-free hole recombination would allow precise determination of the forbidden band gap. Unfortunately, the free-free transition has not yet been observed in GaAs (Ref. 28:386). Therefore, band gap energy estimates currently are based upon observed exciton transitions.

Line 2 in Figure 1 depicts the energy state transition involved in the annihilation of a free exciton. An exciton may be thought of as an electron loosely bound to a hole in a manner similar to an electron in the hydrogen atom. In GaAs at 2° K, the annihilation of a free exciton results in an emission at 1.5156 eV. The full width at half maximum of the free exciton emission is approximately 1 meV. The energy and shape of this line are independent of impurity concentration (Ref. 28:387). A formula for calculating

the energy released during free exciton annihilation is given by Pierce (Ref. 21:38), among others. This energy depends upon the binding energy of the exciton and the kinetic energy of the center of mass of the exciton as well as the band gap energy.

Line  $3_A$  of Figure 1 illustrates the energy transition involved in the annihilation of an exciton bound to a donor site. Line  $3_B$  is for an exciton bound to an acceptor site. These bound excitons emit lower energy photons than do free excitons. The primary energy difference is due to the binding energy between the exciton and the donor or acceptor site. According to Williams, and Bebb (Ref. 28: 341-351), it is believed that excitons can be bound to both neutral and ionized donors in GaAs. Excitons bound to neutral acceptors are believed to exist as well, but in GaAs, excitons bound to ionized acceptors are considered unlikely. In silicon doped GaAs (GaAs:Si), at  $2^{\circ}$  K, three bound exciton lines have been reported. They are:

- 1) exciton bound to neutral donor-----1.5145 eV
- 2) exciton bound to ionized donor-----1.5135 eV
- 3) exciton bound to neutral acceptor----1.5125 eV

(Ref. 28:342). Bound excitons have no kinetic energy associated with their centers of mass. Since variations

in kinetic energy are responsible for the broadening of the free exciton emission line, bound excitons have slightly narrower lines than free excitons. The relative intensity of the bound exciton lines depends somewhat upon temperature and impurity concentration (Ref. 28:343).

Transition  $4_A$  in Figure 1 illustrates a free electron-bound hole recombination. The energy associated with this transition is:

$$E = E_G - E_A + kT \pm nE_p \quad (2)$$

where

$E_A$  = acceptor energy level, 30 meV in a GaAs:Si,  
@ 20° k (Ref. 27:1289)

$n$  = number of phonons which assist the transition

$E_p$  = phonon energy, 36 meV for the longitudinal  
optical phonon in GaAs (Ref. 28:388)

The last term in equation (2) represents the discrete amount of energy that can be given to or absorbed from the crystal in the form of lattice vibrations. Energy is usually given to the crystal and phonon replicas are generally observed only on the low energy side of the zero phonon peak. The third term in equation (2) accounts for the kinetic energy of the free electron. This term increases with increasing temperature. At the same time, however, the band gap energy decreases with temperature. Between 21 and

55° K the magnitude of the decrease in band gap is nearly equal to the increase in  $kT$  and so little change should be expected in the peak energy of the free electron-bound hole recombination in this temperature range. Above 55° K, however, the band gap energy decreases faster than  $kT$  increases and one would expect to observe a shift of this peak to lower energies with increasing temperatures but not as great a shift as is seen in  $E_G$ . Also, since the kinetic energy of the free electrons is actually distributed around  $kT$  and since the deviation in kinetic energy grows as the average temperature increases, this peak should broaden slightly with increasing temperatures. At 20° K, the photon released from the zero phonon free electron-bound hole recombination in GaAs:Si should have an energy of approximately 1.493 eV.

Transition  $4_B$  represents a bound electron-free hole recombination. The photon emitted from this transition obeys a formula similar to equation (2) but with the acceptor energy level,  $E_A$ , replaced by the donor energy level,  $E_D$ . In GaAs:Si,  $E_D = 6.80$  meV (Ref. 28:342) and therefore, the bound electron-free hole transition will result in a higher energy photon than the free electron-bound hole recombination,  $E = 1.516$  in GaAs:Si at 20° K. The temperature dependence of the energy peak and line width will be similar for both types of transition.

The final transition depicted in Figure 1 represents a bound electron-bound hole recombination. The transition energy in this case is given by (Ref. 28:335)

$$E = E_G - (E_A + E_D) + e^2/\epsilon R \quad (3)$$

where

$e$  = the charge on an electron

$\epsilon$  = the dielectric constant of the medium (GaAs)

$R$  = the spacing between the interacting donor  
acceptor pairs

Since the donors and acceptors must occupy lattice sites,  $R$  takes on discrete values in an ideal crystal and a series of sharp lines might be expected from these transitions. A series of sharp luminescence lines corresponding to individual pairs has been observed in GaP, but Gershenson (Ref. 6) has proposed that sharp lines will not be observed for simple centers in GaAs because the activation energies of the donors and acceptors are too small. As a result, for electron-hole pairs with values of  $R$  small enough to have resolvable energy differences, the energy of the recombination would be above the band gap energy. The only bound-bound luminescence yet observed in GaAs is the distant pair limit where  $E = E_G - (E_A + E_D)$ . For GaAs:Si, this line appears at approximately  $E = 1.485$  eV, at  $20^\circ$  K.

In summary, luminescence from simple centers in GaAs occurs at energies near the band gap energy of 1.521 eV. Free and bound excitons and the bound electron-free hole recombination occur at approximately 1.51 eV. while free electron-bound hole and bound electron-bound hole recombinations occur at approximately 1.49 eV. The relative intensity and shape of most of these lines depends upon temperature and impurity concentration. Since many of the lines are so near the same energy, they are often difficult to resolve. GaAs often contains several different contaminants which introduce different donor and acceptor levels. All this makes it difficult to identify exactly which mechanism and which type of impurity is responsible for the observed luminescence.

#### Complex Centers

Luminescence is often observed in GaAs, and most other crystals, at energies which are too low to be explained in terms of simple centers. Such luminescence is assumed to result from complex recombination centers. Complex centers are frequently referred to as deep centers because their energy levels are located much deeper into the forbidden band gap than the energy levels of simple (shallow) donors and acceptors. Complex centers are almost always attributed in full or in part to lattice vacancies although

some have been attributed to the presence of transition metals (Ref. 28:359) and to precipitates (Ref. 16:10).

Vacancies are believed to act as donors or acceptors. In GaAs, for example, a Ga vacancy acts as an ionized acceptor (Ref. 28:373) while an As vacancy is an ionized donor (Ref. 13). In addition, these vacancies disturb the periodicity of the potential energy in the lattice and thereby give rise to localized perturbations in the band gap and the energy levels within the gap. Furthermore, these vacancies can interact with themselves or with impurities to cause additional variations in the energy levels. For example, if an As vacancy (an ionized donor) were located in the vicinity of an acceptor impurity, the two might interact via coulombic attraction to form a molecule-like complex (Ref. 29:1663). This pseudo-molecule might have its own unique ground and excited energy states which might appear to be deep within the forbidden gap. In some samples, similar interaction may occur between Ga vacancies (ionized acceptors) and As vacancies (ionized donors).

Several transitions from complex centers in GaAs have been identified. Some of these transitions and the centers generally believed to be responsible for them are listed by Lusk (Ref. 16:10). Although many studies have

been completed, little is really known about most of these deep level transitions and there is no well developed theory to explain all their properties.

The most common characteristic of complex center luminescence, aside from low energy, is broad line width. One theory which accounts for at least part of this broadening is depicted in Figure 2. The theory depicted includes both variation of the electrostatic potential due to charged impurities and vacancies, and the formation of band-tail states. In this model, shallow donor and acceptor energy levels are indistinguishable from the perturbed conduction band and valence band respectively. Deep level acceptors, however, remain distinguishable and follow the fluctuations of the valence band energy. The energy level fluctuations predicted in this model are completely random, but the magnitude of the fluctuations should depend somewhat upon the concentration of ionized impurities and defects. As illustrated in Figure 2, the exact energy of a particular transition depends in part upon the position of the electron-hole pair. This is believed to account for the broad line width of emission from complex centers.

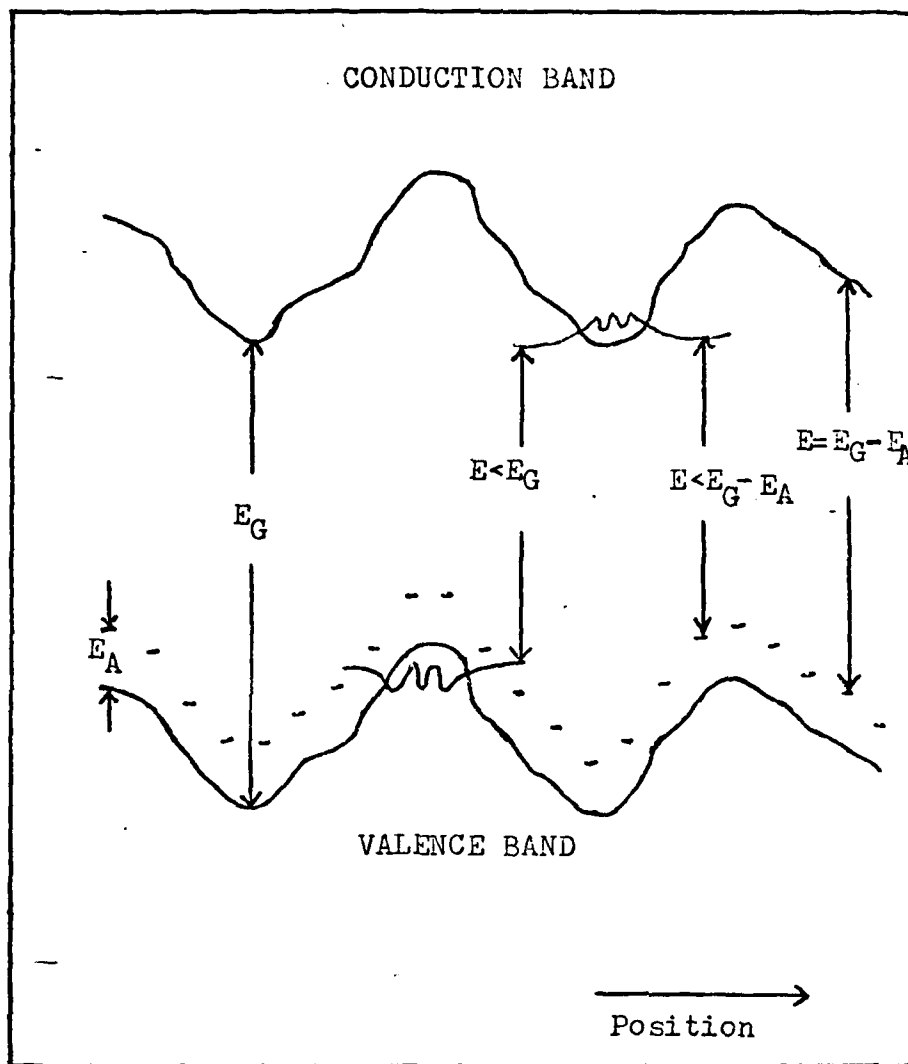


Figure 2. Perturbed Energy Band Diagram (Ref.23)

Two broad emission lines frequently observed in GaAs:Si are of particular interest in the thesis. The first is centered at approximately 1.44 eV and the other is centered at approximately 1.36 eV. Both luminescence bands are very broad (40 to 100 meV) and their peak energies and band widths generally depend upon temperature (Ref. 8, 11, 12, and 23), excitation intensity (Ref. 1 and 23), and silicon concentration (Ref. 11, 12, 20, 23, and 25). An increase in temperature or silicon concentration or a decrease in excitation intensity has been observed to lower the peak energy and increase the half width of these two emissions.

Several different complexes have been proposed as sources of these emissions. The 1.44 eV band is commonly attributed to a center involving an arsenic vacancy and silicon acceptor ( $V_{As} - Si_{As}$ ), (Ref. 2, 9, and 29). Many other authors (Ref. 11, 12, and 25), have simply attributed the band to a deep acceptor level introduced by silicon. It has also been suggested (Ref. 2 and 23) that this band is due to a complex of silicon occupying nearest neighbor Ga and As sites ( $Si_{Ga} - Si_{As}$ ). Others (Ref. 14:4484, and 22), however, have suggested that these nearest neighbor complexes should be electrically and optically inactive. Those authors who attribute the band to a deep acceptor level seem to be alluding to a complex of some kind but

they do not speculate as to the exact nature of the complex. All the authors referenced above agree that the 1.44 eV band results from a silicon acceptor ( $\text{Si}_{\text{As}}$ ) bound to a donor. There is some disagreement over the nature of this donor but an arsenic vacancy ( $\text{V}_{\text{As}}$ ) seems most probable.

The 1.36 eV band is also attributed to a deep silicon acceptor level (Ref. 2, 3, 11, and 15). Again, the most common explanation is a silicon acceptor in association with an arsenic vacancy but no explanation has been found for why the same complex ( $\text{V}_{\text{As}} - \text{Si}_{\text{As}}$ ) is responsible for two different emission bands.

#### Electron Penetration Depths

One way to induce luminescence in a crystalline semiconductor is to excite it by bombarding the crystal surface with a beam of energetic electrons. The electrons penetrate the crystal and lose their kinetic energy through collisions with the electrons in the crystal. The energy given up by the beam of electrons causes transitions to excited energy levels in the crystal. The electrons and holes quickly transition back to their ground energy states and, in the process, emit radiation. Luminescence produced in this way is called cathodoluminescence.

When one is interested in the variation of luminescence with depth into the crystal, it is important to know the penetration depth of the exciting electrons. The penetration depth of the electrons indicates the approximate thickness of the surface layer that is being sampled.

Penetration of electrons into various materials has been studied extensively, however, most data is for high energy ( $>5$  keV) electrons at normal incidence. Feldman (Ref. 5), studied penetration depth of 1-10 keV electrons in solids (mostly metals), at normal incidence. He was able to fit his data to an equation of the form:

$$R = bE^r \quad (4)$$

where

$R$  = the penetration

$E$  = the energy of the electrons in keV

and  $b$  and  $r$  are constants related to the material being bombarded

Martinelli and Wang (Ref. 17) studied penetration of normally incident electrons with energies of 3-7 keV into GaAs. Their data was also fit to equation (4) and they determined that for GaAs,  $b = 270 \text{ \AA}$  and

$r = 1.46$ . Rosenstein (Ref:24) found that electrons incident on Polystyrene at  $45^\circ$  lost more of their energy closer to the surface than did normally incident electrons but that the total penetration ranges were within 10% of each other. Making the approximation that the range of electrons incident at  $45^\circ$  is equal to the penetration range of normally incident electrons, and substituting Martinelli and Wang's numbers into equation (4), one can easily estimate the penetration range of electrons incident on GaAs at  $45^\circ$ . Using this approach, one finds that 1500 eV electrons penetrate approximately 490 Å and 900 eV electrons penetrate approximately 230 Å.

#### Laser Beam Penetration

A 15 mW Helium-Neon (He-Ne) laser was used as a secondary excitation source. Therefore, it is necessary to know the approximate penetration depth of light from the He-Ne laser for the reason mentioned above. Transmission of light through a medium is governed by Beer's law,

$$I(x) = I(o)e^{-\alpha x}$$

where

$I(x)$  = intensity of the light as a function of  
the distance into the medium

$I(0)$  = intensity of the light at  $x = 0$   
 $e$  = base of the natural logarithm  
 $\alpha$  = the absorption coefficient of the  
           material at the wavelength of interest  
 $x$  = distance into the medium

From Sturge (Ref. 26:772), the absorption coefficient of GaAs at a wavelength of 6328 Å is  $3.7 \times 10^{-4} \text{ cm}^{-1}$ . Therefore, the intensity of the He-Ne light will be reduced to  $1/e$  times its initial value at a penetration depth of 2700 Å. This is also the penetration depth reported for He-Ne light in GaAs by Namba, et al (Ref. 19:1340).

#### Ion Implantation

Ion implantation is the most commonly used method of introducing donor and/or acceptor impurities into GaAs. Implantation is a relatively simple concept. Atoms of the desire impurity are ionized and accelerated to very high energies. These high energy ions then bombard the sample that is to be implanted. When these ions impact the surface of the sample, some atoms are knocked out of the material and some of the ions bounce off the surface, but most penetrate into the crystal and are trapped.

Ion implantation has several advantages over other doping techniques. By controlling the energy and shape of

the beam of bombarding ions, fairly precise, three-dimensional control of the concentration of dopant can be achieved. Ion implantation can be used with virtually any impurity species. Implantation does not have to be accomplished at the time of crystal growth and it does not involve extremely high temperatures as do some other doping methods. Implantation does, however, cause severe damage in the surface of the crystal. This damage must be reduced by annealing before the semiconductor is useful.

Three of the GaAs samples used in this study were ion implanted with silicon. A brief discussion of range theory for implanted ions is presented here to aid in understanding the characteristics of the samples used.

A range distribution theory developed by Lindhard, Scharff, and Schiott (LSS) is the universally accepted theory for predicting implantation depths and distributions. The theory was developed for implantation into amorphous solids but has been adapted to crystalline solids as well. The LSS theory predicts the density of implanted ions as a function of distance into the surface based upon the total number of ions per unit area striking the surface, the energy of the ions, the mass of the ions, and the density of the solid. The details of this theory are clearly described in a lengthy work by Gibbons (Ref. 16), and further discussion of the theory is not deemed necessary in this thesis.

The implanted samples used in this investigation were implanted with 120 keV silicon ions. Two samples received a dose of  $10^{14}$  ions per square centimeter and a third received  $10^{15}$  ions per square centimeter. Figure 3 shows the theoretical concentration distribution for 120 keV silicon ions in GaAs over the appropriate range of total ion dosage. These curves do not account for the diffusion of ions during the annealing process that followed the implantation. Diffusion would be expected to flatten the peaks of the curves in Figure 3 slightly.

#### Ion Etching

Ion etching is essentially sand blasting on an atomic scale. It is widely used in industry for cleaning and polishing surfaces and is being used more and more for very precise etching of surfaces. The fundamental process involved in ion etching is the transfer of momentum from the incident ions to the atoms of the target. If enough momentum is transferred to an atom of the target, it will leave the surface and in this manner, the surface is etched away. One major disadvantage of ion etching is that not all the energy of the bombarding ions goes into removing atoms from the surface. Some of this energy is lost in the creation of surface disorder. In the case of crystalline targets, the lattice may be nearly destroyed in a thin layer of surface.

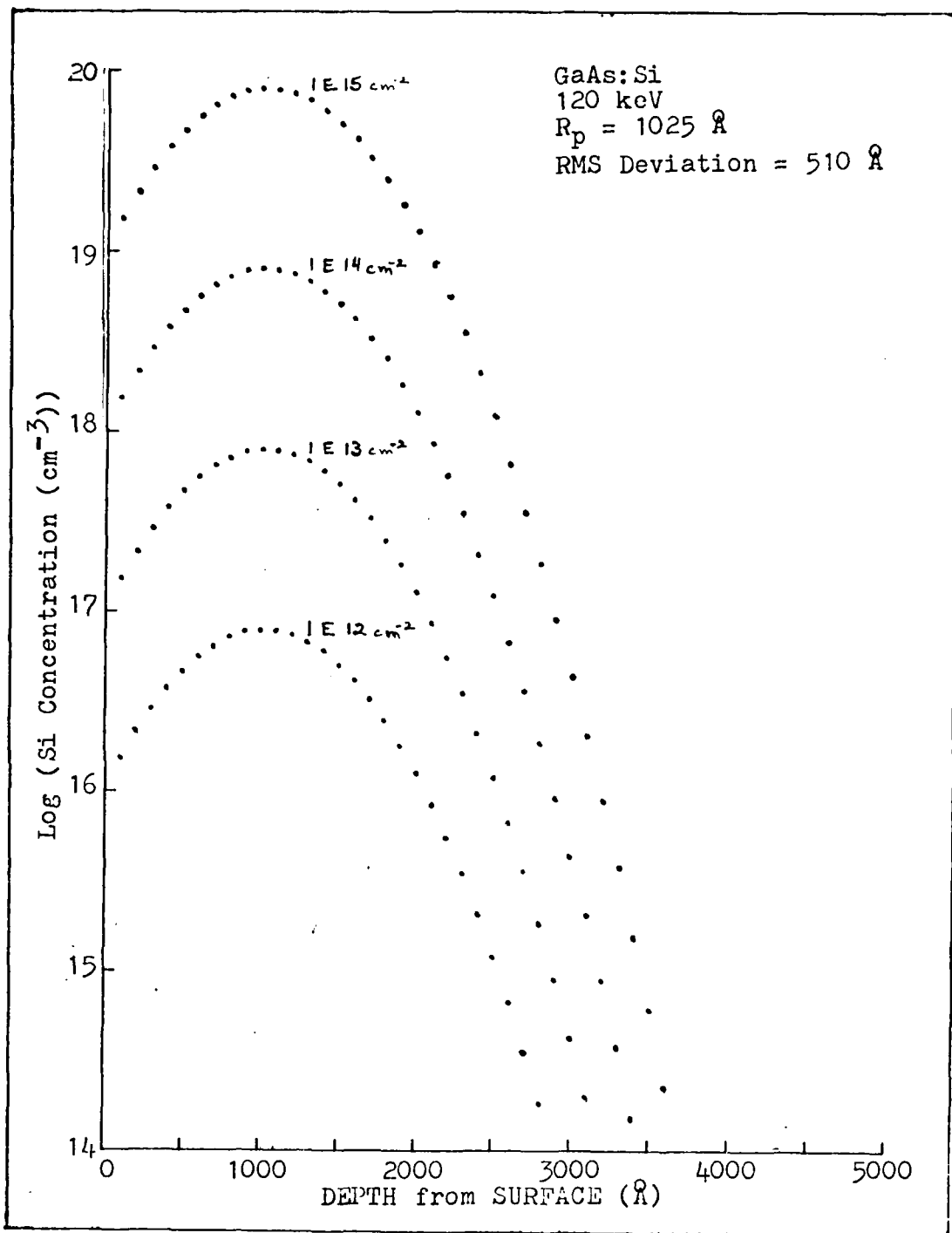


Fig. 3. Theoretical Ion Implantation Range Distribution  
(Courtesy: Capt. G. Pomrenke, AFAWL/AADR)

Kawabe, et al (Ref. 10:2556-2561), studied the effects of ion etching on the properties of GaAs. Figure 4 illustrates the observed dependence of etch rate upon ion energy and ion current. Figure 4 illustrates that for a normally incident ion beam at constant current, etch rate is not a linear function of ion energy. On the other hand, etch rate does appear to be nearly linearly dependent upon ion current density. The etch rate of GaAs with normally incident (incidence angle =  $0^\circ$ ), 500 V argon ions, was found to be approximately 0.8 Å/min per unit ion current density (in  $\mu\text{A}/\text{cm}^2$ ). Kawabe, et al, studied the lattice damage caused by ion etching through helium backscattering analysis and photoluminescence. Their helium backscatter data indicated that etching GaAs with 100 eV and 2 keV  $\text{Ar}^+$  produced nearly amorphous surface layers 23 Å and 72 Å thick respectively. Their depth-resolved photoluminescence data was taken using a He-Cd laser as the excitation source and anodic oxidation for surface layer removal. This laser penetrates approximately 100 Å into GaAs. The photoluminescence data indicated that in addition to the amorphous surface layer, ion bombardment caused what they termed a defect diffused layer approximately 2000 Å thick for both 100 eV and 2 KeV Ar ions. These defects were presumed to exist and produce non-radiative and new radiative recombination centers because

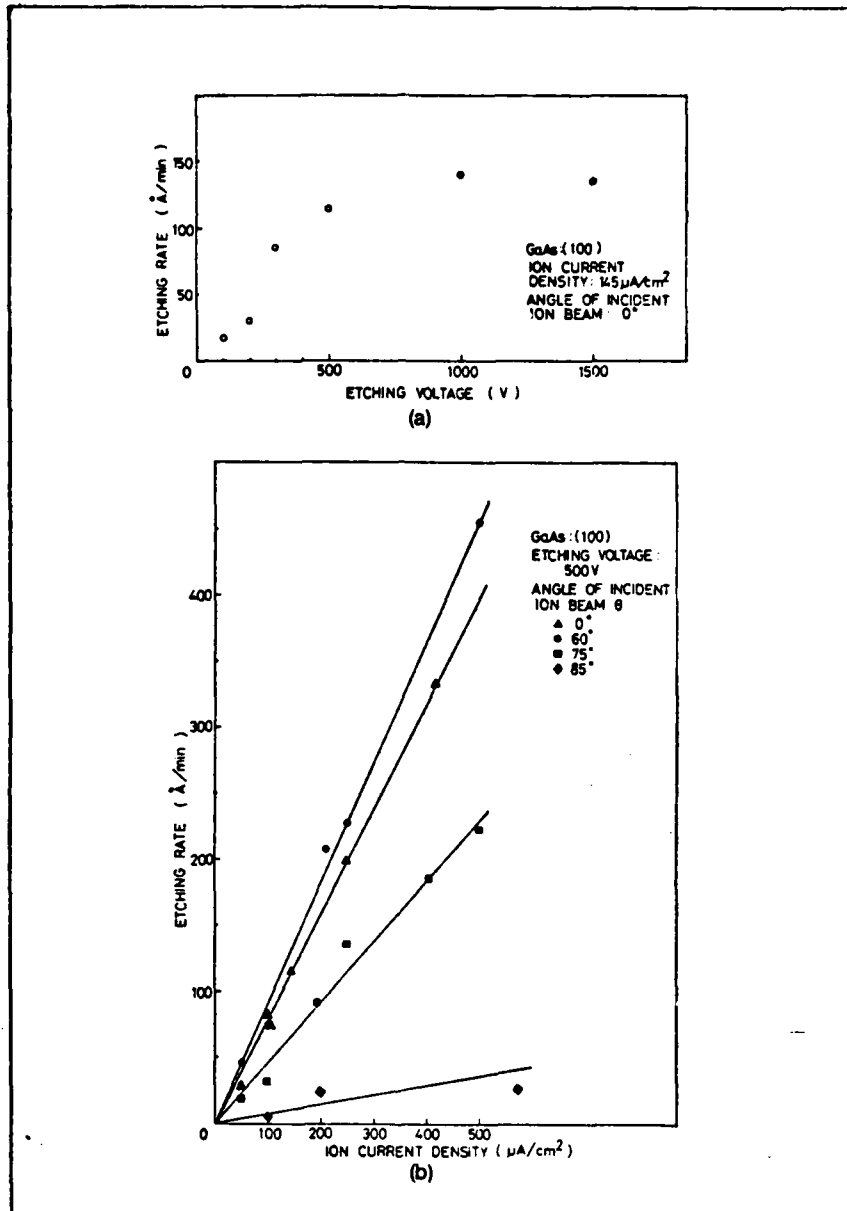


Fig. 4. Dependence of Etch Rate on Ion Energy(a) and Ion Current(b) (Ref:10)

the ion etching resulted in severe (>80%) reduction in the intensity of a spectral line which they found at 8317 Å (1.491 eV) and, at some depths, the appearance of a new peak at 8390 Å (1.478 eV).

McGuire (Ref. 18), presents an excellent theoretical discussion and Auger spectroscopy data on the effects of ion sputtering on III-V semiconductor surfaces with emphasis on the phenomenon of preferential sputtering. The effects of the relative masses of the sputtering ions and the target atoms is discussed. As stated earlier, the basic principle involved in ion etching is momentum transfer. Since the momentum transfer cross section is greatest for two particles of the same mass, all other relevant factors being held equal, light ions will transfer momentum to Ga more effeciently than to As. Therefore, bombardment of GaAs by light ions such as He, Ne, and Ar should result in an As rich surface while bombardment by heavier ions such as Kr or Xe should result in a Ga rich surface. McGuire, in fact, found that bombarding GaAs with 500 eV Ar ions produced a surface that was 56.5% As instead of its normal 50% (Ref. 18:140). It was also found that implantation of the low energy ions may be a problem that affects surface composition. It was found that Ar atoms, though not bound chemically, appear to preferentially displace Ga atoms in the lattice (Ref. 18:144).

McGuire makes the above observation with no further explanation. It would seem that while argon atoms are not bound chemically, positive argon ions, which are usually used in etching rather than neutral atoms may, in fact, tend to form ionic bonds with As and thus chemically displace the Ga.

### III. Experiment

The objectives of this thesis were to establish ion etching and induced luminescence techniques for studying damaged surfaces and then to use these techniques to characterize selected GaAs surfaces. In order to meet these objectives, a system was assembled which allowed excitation, detection, and recording of the cathodoluminescence and photoluminescence from a sample of GaAs. The system assembled also allowed in-situ ion etching of the sample. Once the system was assembled, procedures were developed for performing the ion etching and luminescence measurement and recording. In this chapter, the system and those procedures are discussed in detail.

#### The System

The system assembled during this research project was built around a large volume, very-high-vacuum chamber which provided the proper environment for ion etching and excitation of cathodoluminescence. A schematic diagram of the system is shown in Figure 5. The chamber held a sample holder which could be cooled to near liquid helium temperature, an ion bombardment gun used in the ion etching, and an electron gun used to excite the sample. Faraday cups were installed inside the chamber on a translating

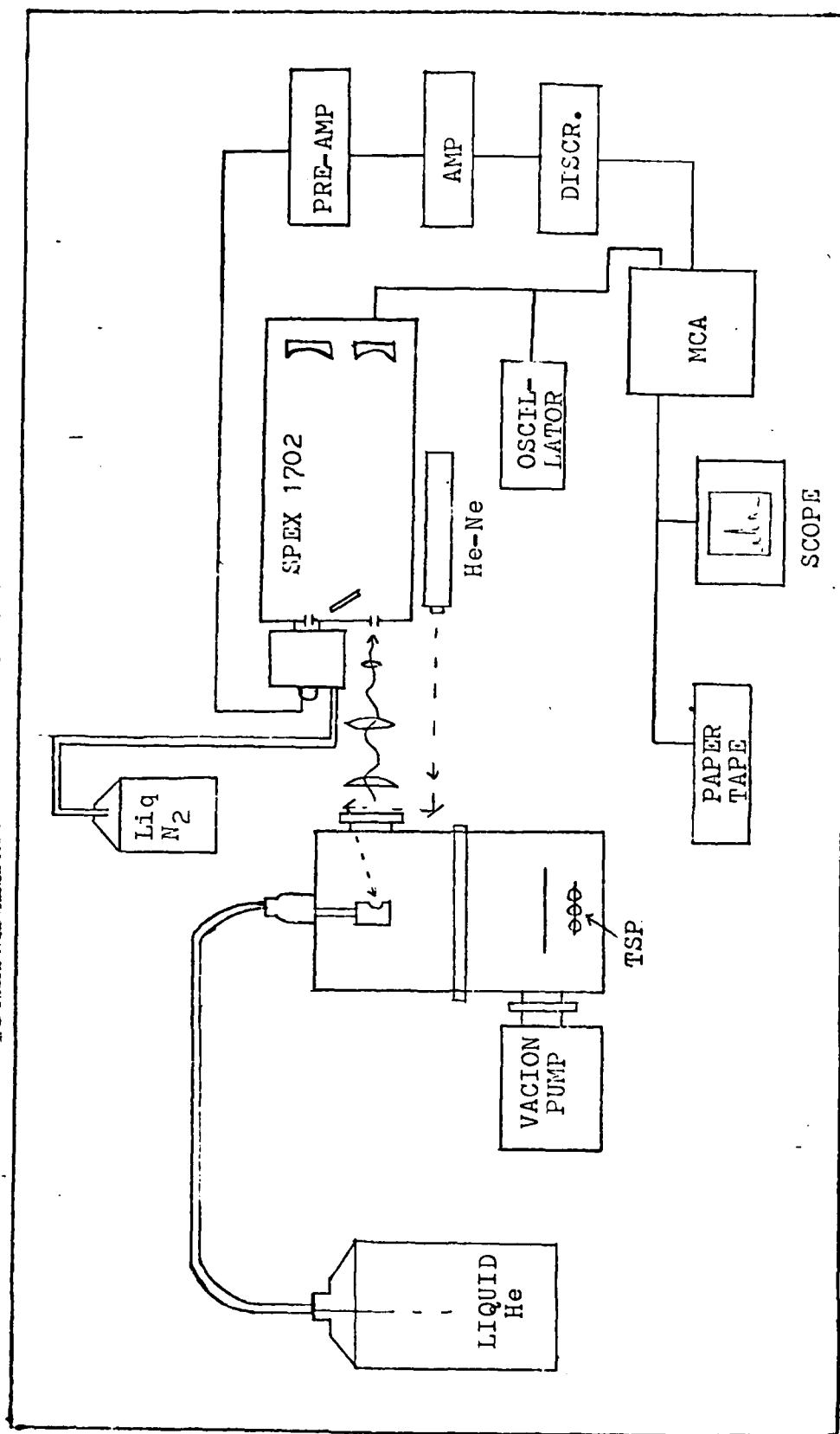


Fig. 5. Luminescence Measuring System Schematic

support so that the ion beam and electron beam currents could be monitored. The system also included a He-Ne laser which was used as a secondary excitation source. A system of three lenses was used to collect the luminescence from the sample and focus it onto the slit of a grating spectrometer. The radiation passing through the spectrometer was detected by a cooled photomultiplier (PM) tube. The output pulses from the PM tube were amplified and sent through a voltage discriminator to block low voltage noise pulses before being recorded by a multi-channel analyzer (MCA). The data, temporarily stored in the MCA, was displayed on an oscilloscope for immediate analysis and if desired, could be transferred to paper tape for permanent storage. Each piece or subsystem of this system is discussed in turn below.

Vacuum System. The vacuum system consisted of a large chamber, 12 inches in outside diameter and approximately two feet deep, and three separate vacuum pumping systems. The chamber was divided into an upper chamber and a lower chamber. A top view of the upper chamber is shown in Figure 6. It had one access port in the center of the top of the chamber where the sample holder was fed through and eight access ports around its circumference. A large port in the front with an eight inch diameter flange contained a seven inch quartz window through which the

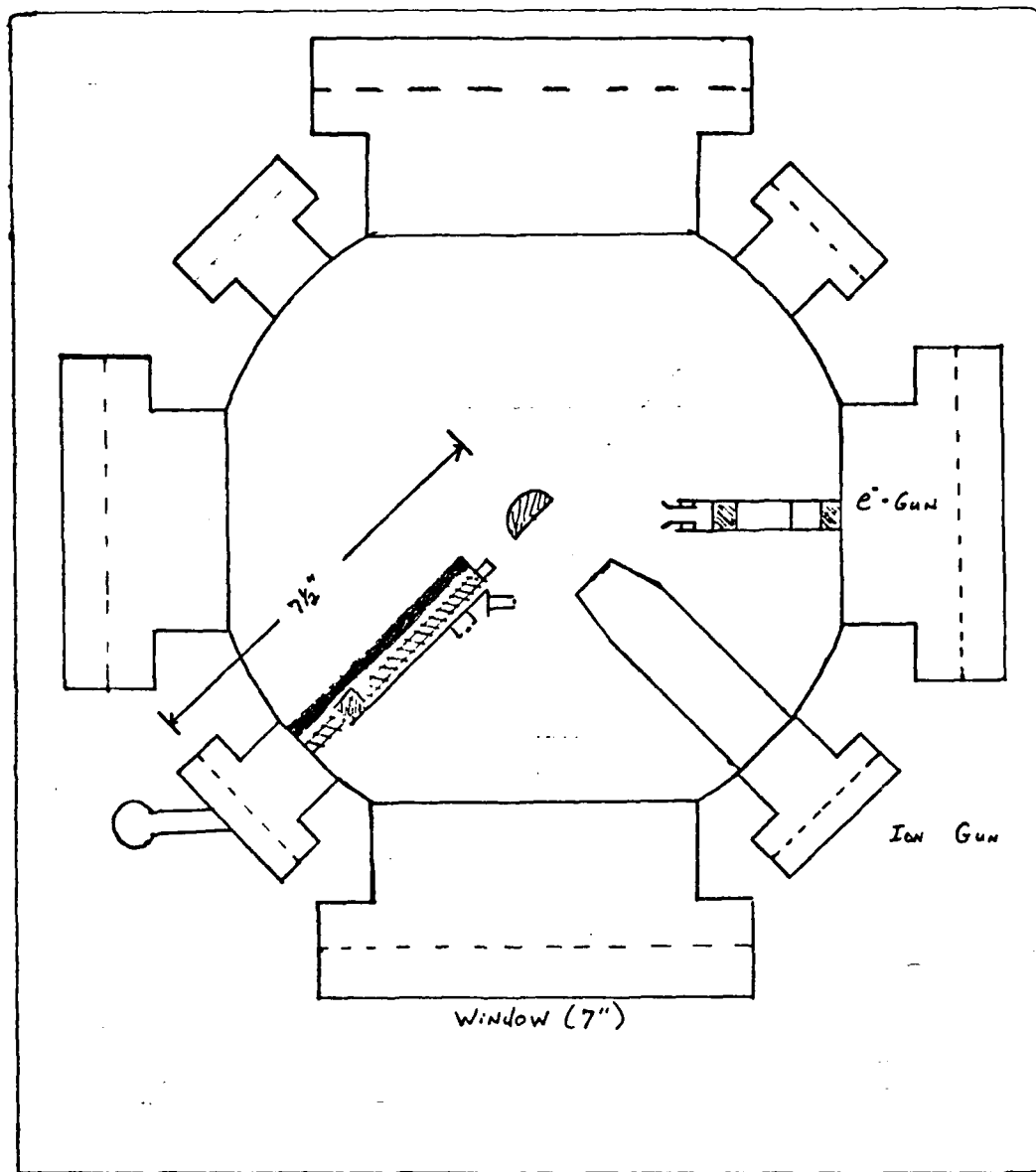


Fig. 6. Vacuum Chamber, Top View

sample was viewed and luminescence was collected. When used, a laser beam also entered the chamber through this window. Located at  $90^{\circ}$  counterclockwise from this window was a six inch diameter flange which held the electrical feedthrough for the electron gun used to excite the sample. The Varian model 981-2043 ion bombardment gun was mounted at a small port located  $45^{\circ}$  counterclockwise from the window. A translating, mechanical support was attached to the small port located  $45^{\circ}$  clockwise from the window. An electrical feedthrough was attached to the port located at  $135^{\circ}$  clockwise from the window, and the remaining three ports were not used.

The lower chamber held a ring of ten small ports with standard 2-3/4 inch diameter flanges. Two of these ports were used, one for the electrical connections for an ionization gauge and one for a leak valve connected to a supply of high purity argon. The lower chamber also contained three special ports. One large diameter port in the back connected the chamber to the primary pump, a Varian model 921-0041, 110 liter/sec noble vac-ion pump. One small port on the right side held a high vacuum valve which opened to pressurize the chamber or to allow rough pumping by two attached vac-sorb pumps. The third special port was located on the left and held the base of a titanium sublimation pump. This system readily achieved and held a vacuum of  $5 \times 10^{-8}$  torr.

Sample Holder. The sample holder which was mounted in the top of the chamber extended down to the point where the sample was mounted in the same horizontal plane as the window, the ion gun, the electron gun, and the Faraday cups. The sample mount itself was a solid block in the shape of a half cylinder. The sample was held to the flat face of the mount with a copper mask that was bolted to the mount. The mask had a 5 mm diameter hole in it through which all but the corners of the sample were visible. The sample mount also held a GaAs diode, a gold-chromel thermocouple and a resistance heater. The diode was used as a temperature sensing unit and was connected to a temperature controller. The heater was used to control the temperature of the sample mount. The thermocouple was attached to an Instrulab series 5000 digital temperature indicator. The sample mount was connected to the end of an Air Products and Chemicals, Inc. model LT-3-100 liquid transfer Heli-Tran. Either liquid nitrogen or liquid helium could be flowed through the Heli-Tran to cool the sample. When liquid nitrogen was used, the temperature indicated by the thermocouple reached  $77^{\circ}$  K. The thermocouple indicated approximately  $8^{\circ}$  K when liquid helium was used.

Ion Bombardment. The ion bombardment gun used was a Varian model 981-2043 with a Varian model 981-2046

power supply and control unit. The gun produced ions with energies of 20 eV to 3 keV, and under optimum conditions, it should have produced a mono-energetic beam with a spot size of approximately 2.5 mm. The gun used electrostatic deflection to move the beam  $\pm 5$  mm in both the x- and y- directions at a distance of two inches from the end of the gun. The gun also had a scan capability which was supposed to allow the beam to be scanned over an area of one square centimeter, again at a distance of two inches from the end of the gun. The gun was pointed directly at the sample. Unfortunately, the end of the gun was less than 1.5 inches from the surface of the sample while the minimum distance specified in the gun manual for proper gun operation was two inches. The gun could not be moved back without major modification of the vacuum chamber or the gun because the inside diameter of the port in which the gun had been installed was slightly less than the diameter of the shield-covering the end of the gun. This was believed to have caused a beam focusing problem which will be discussed further in the results section of this thesis.

Electron Gun. The electron gun used as the primary excitation source in this thesis project was a Superior Electronics Corporation Type SE-3M electron gun. The gun design featured an indirectly heated cathode and

electrostatic deflection plates. The power supply for the heater filament was floated at the same potential as the cathode and voltage for deflection plates was provided by six, 45 volt drycells connected in series. The series of drycells was grounded between the third and fourth cells, thus providing approximately  $\pm 135$  V for the deflection plates. The gun provided zero to 1500 eV electrons, and at 1500 eV, electron currents of up to 100 microampers ( $\mu$ A) were obtained. Typically, the gun was operated at 900 or 1500 eV and 50  $\mu$ A.

Laser. A Spectra Physics model number 124A, 15 mW He-Ne laser was used as a secondary excitation source. The laser was positioned on a table in a convenient location and the beam was deflected by two mirrors through the window in front of the vacuum chamber onto the sample. No attempt was made to either expand or focus the beam, nor was the power density on the sample estimated. No provisions were made to vary the power density on the sample.

Beam Detectors. Two simple Faraday cups were assembled and installed inside the chamber on a horizontal translating support as shown in Figure 6. A Faraday cup approximately one centimeter in diameter was oriented perpendicular to the ion gun and by turning the handle of the translating support it could be moved

directly into the ion beam. The cup consisted of a collector and a grid to suppress secondary emission of electrons. It also included two wires oriented perpendicular to each other that could be grounded either directly or through an ammeter. They were intended to be an aid in aiming and focusing the beam but proved to be ineffective primarily because the cup was too close to the end of the ion gun. The second Faraday cup was oriented so that it could be moved directly into the electron beam. This cup had only two elements, a collector and a grid for suppressing secondary electron emission. Using these two Faraday cups, both the ion beam and the electron beam currents could be measured without moving the beams. The electron beam had to be refocused slightly, however, to obtain a correct measurement due to the position and small diameter of the cup used to measure it. Neither of these cups were of much value in aligning the ion beam and focusing it onto the target.

In order to properly align the ion beam, a third detector was built. This detector was mounted directly onto the sample holder as shown in Figure 7. The detector was simply a plate which was insulated from ground. By connecting the plate to ground through a microammeter the ion current hitting the plate could be

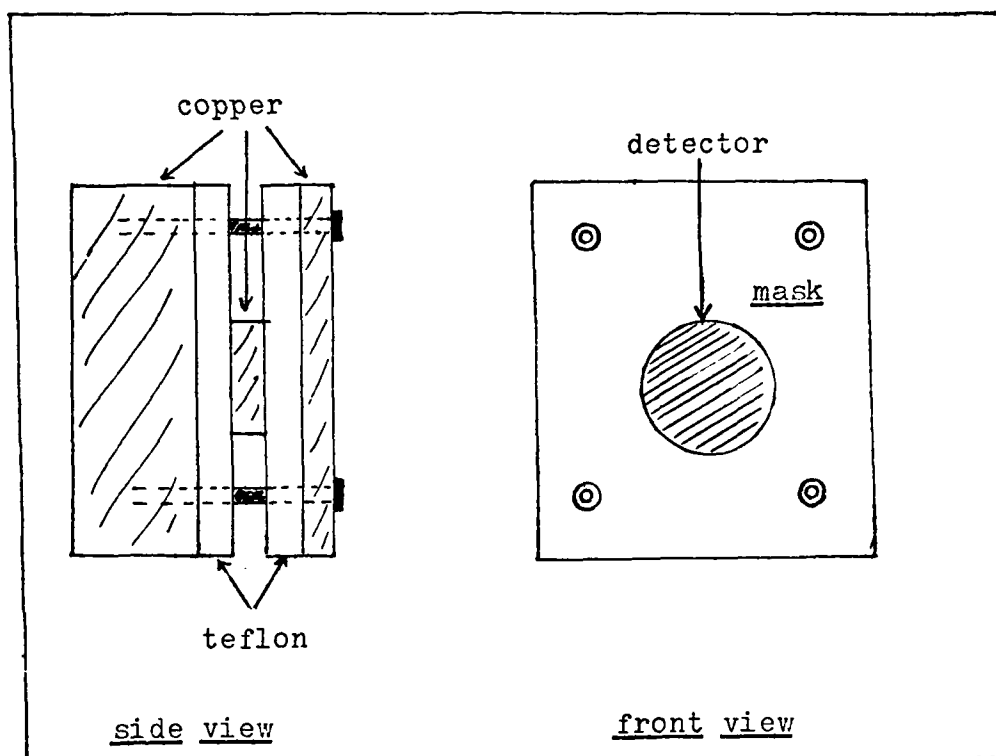


Fig. 7. Ion Detector

measured. This plate was held in place by the same mask which held the sample but had to be insulated from the mask because the mask was grounded. This assured that the detector was in the same position as the sample would be. With this arrangement, the ions hitting the detector produced a current through the microammeter, those ions that hit the mask did not affect the current through the microammeter. The current measured included both the incident ions and the secondary electrons emitted and therefore, was not an accurate measurement of the ion current on target. The current through the microammeter did, however, reflect the relative magnitude of the ion current hitting the target and the beam was aligned and focused by adjusting the position and focus controls until the measured current was maximized.

Optics. Three quartz lenses were used to collect the luminescence radiated by the sample and focus it onto the entrance slit of a spectrometer. A diagram of these lenses along with the source and the entrance slit of the spectrometer is shown in Figure 8. The first lens was a 140 mm diameter plano-convex lens with a focal length of 250 mm. This lens was placed approximately 280 mm from the sample (about 1.5 inches for the vacuum chamber window). Light emerged from the first lens nearly collimated and entered the second lens which had the same diameter as the first but had a focal length of 150 mm.

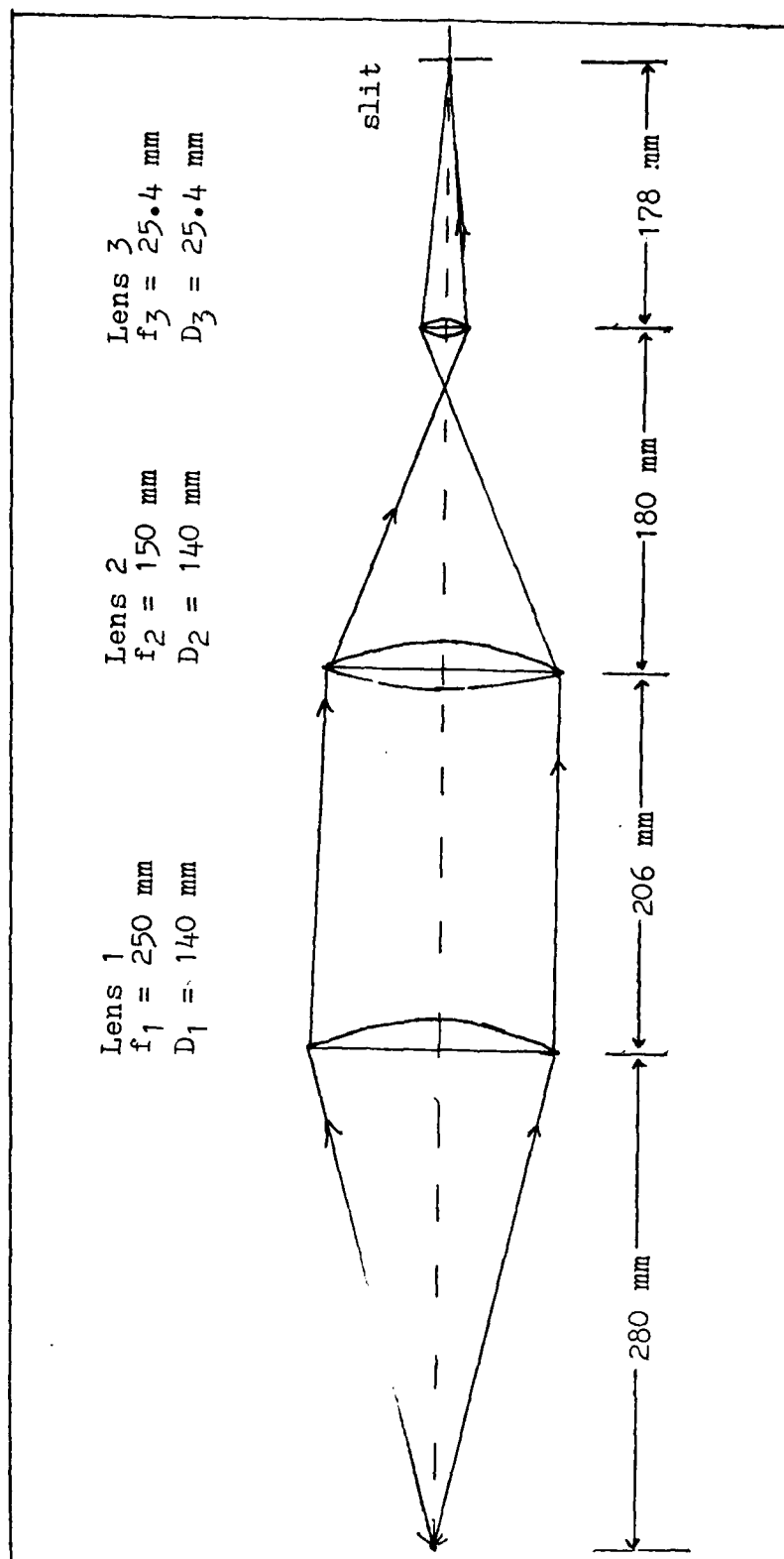


Fig. 8. Optics Arrangement

Light emerging from the second lens converged to a point very near the focal point of this lens. The third lens had a diameter of 25.4 mm and a focal length of 25.4 mm as well. It was positioned approximately 30 mm away from the point where the light coming through lens two was focused. As a result, the light was finally focused approximately 178 mm to the right of lens three which was where the entrance slit of the spectrometer was located. In this configuration, the image distance from lens three divided by the diameter of lens three was equal to seven which matched the  $f/\#$  of the spectrometer.

Spectrometer. The spectrometer used in this thesis project was a Spex Industries, Inc.' model 1702, three-quarter meter Czerny-Turner spectrometer with a Bausch & Lomb diffraction grating having 1200 lines/mm and blazed at 5000 Å. The Spex 1702 featured automatic wavelength scanning that could be driven by either an internal or external stepping motor. The spectrometer had adjustable entrance and exit slits, that could be varied from 5  $\mu$ m to 4 mm and a variable height adjustment on the entrance slit.

Photomultiplier. The luminescence spectra were detected with a cooled EMI 9808B photomultiplier. The EMI 9808B has an S-1 type cathode and 14 beryllium-copper, linear focused dynodes. The tube is sensitive in the 0.3

to 1.1 micron wavelength range. The cathode voltage for the tube was supplied by a Fluke model 404M high voltage power supply. During most of the work in this thesis, the tube was operated with a cathode voltage of -2000 V. The tube was cooled to  $-58^{\circ}$  C by a Products for Research model TE 114 liquid-nitrogen-cooled photomultiplier tube housing and the temperature was maintained by a Products for Research model TE 114 control unit.

Amplifiers and Discriminator. The current pulses leaving the anode of the PM tube were first pre-amplified by a Keithly model 104 wide band amplifier. The PM tube and pre-amplifier were DC coupled through a 100 k-ohm resistor to prevent charging of the input capacitor on the preamplifier. This amplifier provided a voltage gain of approximately 100. From the pre-amplifier, the signal was fed to a Tennelec model TC 200 amplifier. From this amplifier, the signal was sent into a Tennelec model TE 411 single channel analyzer which functioned as a voltage discriminator. The discriminator produced an output pulse whenever it received an input signal above a preset voltage. This prevented low voltage noise pulses from being counted as part of the signal.

Multichannel Analyzer. The output pulses from the discriminator were sent to a Hewlett-Packard series 5400A multichannel analyzer (MCA). The MCA counted the incoming

pulses and recorded the number of pulses counted during 1024 separate blocks of time. The number of pulses recorded in each of the 1024 channels was temporarily recorded in the memory of the MCA. This data was graphically displayed on an oscilloscope, where it could be quickly analyzed, and could also be recorded on paper tape for permanent storage.

### Procedures

This section of the thesis describes the way in which the system was operated to obtain depth resolved luminescence data from GaAs samples. Each of the major steps is described.

Chamber Evacuation. One routine but essential task accomplished during this project was evacuation of the vacuum chamber. The chamber was evacuated from ambient pressure to less than  $5 \times 10^{-3}$  torr with two vac-sorb pumps, which were cooled with liquid nitrogen. With the system sealed up except for the high-vacuum valve between the chamber and the vac-sorb pumps, the valve to one of the vac-sorb pumps was opened. The first pump was left open until the pressure in the chamber reached approximately 1 torr. At that time, the valve on the first vac-sorb pump was closed and the second vac-sorb pump was opened. The second vac-sorb pump usually pumped the system to

$1 \times 10^{-3}$  torr and always less than  $5 \times 10^{-3}$  torr as indicated by a Hastings model 461 thermocouple vacuum gauge attached to the roughing line of the system. The second vac-sorb pump and the high-vacuum valve on the chamber were then closed and the noble vac-ion pump was started. At the same time, the titanium sublimation pump was turned on. The titanium sublimation pump greatly improved the pumping rate of the system. The titanium pump was kept on 100% of the time until the pressure reached  $10^{-6}$  torr. It was operated 50% of the time between  $10^{-6}$  torr and  $10^{-7}$  torr and 25% of the time between  $10^{-7}$  and  $10^{-8}$  torr. Using the above procedure, the system could be pumped from ambient pressure to  $5 \times 10^{-8}$  torr in approximately three hours. The system would not readily achieve lower pressures so it was generally operated at this pressure. The titanium pump was turned off except for periodic runs of two minutes at a time, three or four times per day. When the sample was cooled with liquid helium to near  $8^{\circ}$  K, the sample-mount acted as a pump and reduced the pressure to approximately  $1 \times 10^{-8}$  torr.

Sample Cooling. Most of the luminescence data taken in this project was taken with the sample at approximately  $8^{\circ}$  K. To achieve this temperature, the sample mount was cooled with liquid helium. The output end of the Heli-Tran transfer line, mentioned earlier, was attached to the

cryo-tip housing and the other end was immersed in a dewar of liquid helium. Gaseous helium was initially blown through the line to purge it of any material that might freeze when exposed to liquid helium. This was accomplished by pressurizing the dewar with two psi of helium and keeping the tip of the transfer line above the liquid level for at least one minute. After the line was purged, the tip of the transfer line was lowered into the liquid helium. This generally resulted in a pressure rise in the dewar of up to five or six psi which speeded the cool down process. When the transfer line tip was lowered into the liquid, control valves that controlled the flow of gas through the cryo-tip and shield were fully opened and a cryo-tip heater was plugged in. The flow remained low in the system while the transfer line was being cooled down. This generally took forty-five minutes to an hour. When the line was thoroughly cooled and liquid began reaching the cryo-tip, the gas flow through the shield vent and tip vent increased by nearly an order of magnitude and the sample temperature began dropping rapidly. At this time, the cryo-tip vent and shield vent flow control valves were closed until the ceramic balls that indicated the amount of flow floated at a height of 2 cm above the bottom of their flow tubes. With the flow reduced to this rate, the temperature stabilized at about  $8-9^{\circ}$  K. If the flow

was reduced farther, it tended to surge and resulted in temperature fluctuations. The temperature controller was not used at these low temperatures because it did not produce stable temperatures. The temperature controller was very effective at maintaining  $150^{\circ}$  K during the ion etching procedure. For this procedure, the flow of helium from the tip vent was reduced to practically zero, and the temperature controller was turned on and adjusted to maintain  $150^{\circ}$  K. At this temperature, the controller maintained the temperature to within  $\pm 0.1^{\circ}$  K.

Ion Beam Alignment. A major task in this project was alignment and focusing of the ion beam. In order to insure that the ion beam was focused onto the sample, the detector depicted in Figure 7 was attached directly to the sample mount in the same manner as were the samples. The detector was connected to ground through a Keithley model 153 microammeter, and the ion current on the detector was maximized for a variety of beam energies. During this alignment process and later in the actual use of the ion gun, the chamber was filled to a pressure of  $5 \times 10^{-5}$  torr with high purity argon. During alignment, the ion gun was turned on, the filament emission current was set at 28 mA, beam energy was set to an energy of interest, and the position and focus controls were alternately adjusted until the maximum current was detected. The positions of

the gun controls which resulted in maximum current at each energy were recorded for later reference.

The ion gun had the capability of rastering the ion beam. Rastering was considered important in assuring uniform depth of etch because it was assumed that the current density was not uniform across the ion beam. If the beam were not rastered, the current density variation would result in non-uniform etch rates across the sample. The sample and detector surfaces were each approximately 5 mm in diameter and the ion beam was supposed to focus to a spot approximately 2.5 mm in diameter. Therefore, it should have been possible to raster the beam over a small area with little or no loss in detected current. This, however, was generally not observed. In most cases, the current dropped as soon as the scan voltage was turned on, even at the lowest possible voltage. The scan voltage at which the current began to drop sharply was also recorded for each beam energy.

Ion Etching. Nearly all the ion etching performed during this project was done with an ion beam energy of 500 volts. Higher energies resulted in higher surface damage and at lower energies, the current densities at the target were low and would have resulted in unacceptably slow etch rates. The sample temperature was maintained at 150° K. This temperature was chosen arbitrarily.

It was high enough to prevent condensation of Ar on the sample and still low enough that the sample could be returned to approximately  $8^{\circ}$  K for luminescence measurements quickly. With the temperature stabilized at  $150^{\circ}$  K and the pressure in the chamber at or below  $5 \times 10^{-8}$  torr, the titanium sublimation pump was run for two minutes to assure that a fresh gettering surface existed. Then, the titanium pump and the noble vac-ion pump were turned off. With the pumps off, high purity Ar was bled into the chamber until the pressure reached  $5 \times 10^{-5}$  torr. The Faraday cup used for measuring the ion current was connected to the microammeter, the grid voltage supply was turned on, and the cup was positioned directly in front of the ion gun. The ion gun was then turned on. The filament emission current was set to 28 mA. The beam energy was set to the desired voltage (usually 500 volts), and the position and focus controls of the ion gun were set to the values which had been found to produce the highest current on the sample area at that beam energy. Also, the scan voltage was turned on in most cases and set to 400 volts. This scan voltage was found to reduce the current onto the sample area by about 10% at a beam energy of 500 volts. With the gun running the Faraday cup position was adjusted as required to intercept all the beam, and the current was monitored for about ten minutes

while the ion current stabilized. When the ion current stabilized, the Faraday cup was moved and the sample was etched for the desired length of time. At the end of the etch cycle, the Faraday cup was re-inserted into the ion beam to block the beam and prevent further etching and to again measure the beam current. This current was compared to the current at the beginning of the etch cycle to insure that no significant changes in gun operation had occurred. The process was completed by turning the ion gun off, starting the ion pump, and cooling the sample back down for a luminescence measurement.

Etch depths were not measured until all the planned etches of a sample were completed. At that time, the sample was removed from the vacuum chamber and the etch depth was measured with a Sloan Dektak surface profile measuring system. Average etch rates were estimated assuming that the etch rate was constant during each of the etch cycles.

Electron Beam Alignment. The alignment and focusing of the electron beam was a relatively simple task because the beam produced a visible glow whenever it struck a metal object inside the vacuum chamber. Even at energies as low as 600 volts, the beam produced a blue glow when it struck a stainless steel object or a GaAs sample. A bright orange glow resulted when the beam struck the copper sample mount or mask. The beam could easily be tracked as the

voltages on the electron gun deflection plates were varied and the focus could be adjusted to produce the smallest spot possible.

The current in the electron beam was measured with the Faraday cup discussed earlier. Since the cup was moveable, the beam current could be measured without changing the position of the beam. However, it was necessary to change the focus of the beam slightly in order to collect all the beam current in the small diameter Faraday cup. This did not prove to be a serious problem because the focus control was easily reset.

Spectrometer Alignment. The Spex 1702 spectrometer was mounted on a large wooden table in front of the vacuum chamber. The position and height of the spectrometer were adjusted so that the optic axis of the entrance leg of the spectrometer was aligned with the sample. A 2 mW He-Ne laser was used to aid in this alignment. The laser was mounted so that its beam entered the center of the exit slit of the spectrometer and so that it struck the center of the exit mirror. The laser beam was reflected off the exit mirror onto the center of the grating, which was rotated so that the laser beam was reflected onto the center of the entrance mirror. From here, the beam was reflected towards the entrance slit. When the laser was aligned properly and the grating was rotated at the proper angle, the laser

entered the center of the exit slit and exited through the center of the entrance slit. The position of the spectrometer was then adjusted until the laser beam leaving the spectrometer struck the center of the sample while at the same time, the spectrometer was kept level.

Optics Alignment. As mentioned earlier, three lenses were used to collect light from the sample and focus it onto the entrance slit of the spectrometer. These lenses were mounted on a two foot long optical bench with translating mounts. The lenses were placed in what was believed to be the proper positions along the rail. Light from a He-Ne laser was deflected into the vacuum chamber and onto the sample. The scattered light from the sample was focused onto the entrance slit of the spectrometer. The spectrometer was set to pass the  $6328 \text{ \AA}$  light of the He-Ne laser and a cooled photomultiplier tube was used to detect the scattered light. Fine adjustments were made to the positions of the lenses to maximize the strength of the signal.

Luminescence Measurements. Both photoluminescence and cathodoluminescence data was gathered from GaAs samples in the 8000 to  $9778 \text{ \AA}$  wavelength range. All but two of the meaningful spectra were taken at temperatures between  $8^\circ$  and  $10^\circ \text{ K}$ .

The wavelength advance of the spectrometer and the channel address of the multichannel analyzer were controlled

by the same oscillator and therefore there was an exact linear relationship between the number of Angstroms scanned by the spectrometer and the number of channels accessed by the analyzer. For all the data presented in this thesis, each channel of the MCA represented a wavelength interval of  $1.73611 \text{ \AA}$ . Therefore, by recording a reference line of known wavelength along with the spectra of interest, the wavelength of any unknown line in the spectra could be determined to within  $\pm 1.73611 \text{ \AA}$  by simply counting the number of channels between the line of interest and the reference line, multiplying this number by  $1.73611 \text{ \AA/channel}$ , and adding the wavelength of the known line. The reference line chosen in this work was the  $8006.2 \text{ \AA}$  line of an argon lamp.

To obtain a spectrum, the sample was cooled to near  $8^\circ \text{ K}$ , the excitation source (either the electron beam or the He-Ne) was turned on, and the spectrometer was set to approximately  $7995 \text{ \AA}$ . The spectrometer slits were closed to 5-10 microns, the MCA was placed in the accumulate mode, and the argon lamp was placed in front of the entrance slit of the spectrometer and turned on. The spectrometer was switched to external drive and as the counter passed  $8000 \text{ \AA}$ , the MCA was started. As soon as the Ar reference line was recorded by the MCA, the argon lamp was turned off and moved out of the way, and the

spectrometer slits were opened to 400 microns while the spectrometer and MCA continued to run. The MCA was advanced at a rate of one channel/second so a scan of 1024 channels took approximately 17 minutes. At the end of the run, the MCA automatically stopped and displayed all the data. At that point, the spectrometer and the excitation source were turned off and the spectrum was reviewed. If the spectrum appeared satisfactory, the data was recorded on paper tape. This data was later transferred to computer data cards which were used with a plot routine to obtain the plots appearing in this thesis.

#### IV. RESULTS AND DISCUSSION

In this research project, cathodoluminescence and photoluminescence data was taken from nine GaAs samples. Six of those samples were etched by Ar ion bombardment so that depth resolved luminescence measurements could be taken. In this chapter of the thesis, data on the performance of the ion bombardment gun and luminescence data from five of the samples studies is presented.

All the GaAs samples studied except sample number one were from the same batch of high-purity, high-resistivity material. The material was grown by the Liquid-Encapsulated Czochraski (LEC) method as discussed by Fairman, et al (Ref. 4) and Hobgood, et al (Ref. 7) on the (100) plane of a seed crystal. All samples were chemo-mechanically polished to produce smooth surfaces free of gross defects. Samples 2 through 5 were virgin samples, i.e., they were not intentionally doped or treated in any special way. Samples 6 and 7 were implanted with 120 keV silicon ions with a total dose of  $10^{14}$  ions/cm<sup>2</sup>. Sample 6 was coated with a film of Si<sub>3</sub>N<sub>4</sub> and annealed at 900° C for 15 minutes in a hydrogen gas flow. Sample 7 was not coated with Si<sub>3</sub>N<sub>4</sub> nor annealed. Sample 8 was not ion implanted but was coated with Si<sub>3</sub>N<sub>4</sub> and annealed at 900° C for 15 minutes. Sample 9

was implanted with 120 keV silicon ions at a total dose of  $10^{15}$  ions/cm<sup>2</sup> and was then capped with Si<sub>3</sub>N<sub>4</sub> and annealed at 900° C for 15 minutes. A summary of the samples used and their preparation is presented in Table 1. The luminescence data presented here is from samples 4, 6, 7, 8, and 9.

A brief summary of the ion gun performance is presented first along with some discussion of the performance date. This is followed by luminescence data from the five samples listed above. The first luminescence data discussed is a comparison of cathodoluminescence and photoluminescence from a typical virgin sample. This is followed by depth-resolved cathodoluminescence data from the same sample. Next, the depth-resolved photoluminescence spectra from sample 6, an ion implanted sample, are presented. This data is then contrasted with the depth-resolved cathodoluminescence data from the same sample. Next, the surface cathodoluminescence data is presented for an annealed but unimplanted sample. This is followed by the depth-resolved cathodoluminescence of an implanted but unannealed sample. Finally, a series of data, including some excitation intensity and temperature dependent data, from sample 9, which was doped with an order of magnitude more silicon ions than sample 6, is presented.

Table I  
Sample Summary

Sample #	Implant*	Cap	Anneal
2	None	None	None
3	None	None	None
4	None	None	None
5	None	None	None
6	$10^{14}\text{Si}^+/\text{cm}^2$	$\text{Si}_3\text{N}_4$	15 min @ $900^\circ\text{C}$
7	$10^{14}\text{Si}^+/\text{cm}^2$	None	None
8	None	$\text{Si}_3\text{N}_4$	15 min @ $900^\circ\text{C}$
9	$10^{15}\text{Si}^+/\text{cm}^2$	$\text{Si}_3\text{N}_4$	15 min @ $900^\circ\text{C}$

\* Implant energy, 120 keV

## Ion Gun Performance

Ion gun performance was assessed in terms of ion current on the target at various beam energies and in terms of observed etch rates. Performance of the gun in terms of ion current delivered to the target for beam energies from 16 to 3000 volts is summarized in Table II. The numbers listed under x and Y deflection and focus are the optimum control settings for each beam energy. The scan voltages listed are the maximum voltages which did not result in appreciable (>10%) reduction in measured current. The ion current is the current hitting a  $0.2 \text{ cm}^2$  detector mounted on the sample holder. It should be remembered that this detector had no grid to suppress secondary electrons and therefore, the measured current results from both impacting ions and emitted electrons. As a result, the indicated currents were believed to be approximately 10% higher than the actual ion currents.

In an effort to improve etch depth uniformity, most etching was performed with the scan voltage set at 400 or 500 V. With the gun controls set as specified in Table II for a 500 V beam, the measured ion current at the target was observed to decrease from  $3.5 \mu\text{A}$  to  $3.1 \mu\text{A}$  (about 11%) when the scan voltage was increased from 0 to 500 V. When the current in this same ion beam was measured with the Faraday cup, which has an area of approximately  $0.78$

Table II  
Variation of Ion Current with Beam Energy

BEAM ENERGY (eV).	X DEFL'N	Y DEFL'N	FOCUS	SCAN VOLTAGE (V)	ION CURRENT
3000	0.6	7.6	2.6	0	10 $\mu$ A
2000	0.7	7.4	2.5	0	8.4 $\mu$ A
1000	2.0	7.3	3.4	200	6.15 $\mu$ A
500	2.4	6.4	4.0	200	3.5 $\mu$ A
250	3.8	5.7	6.6	100	1.65 $\mu$ A
100	3.6	5.6	4.1	80	340nA
50	2.1	6.5	0.0	20	37nA
25	0.0	10.0	0.0	20	2.2nA
16	0.0	10.0	0.0	20	1.35nA

Pressure =  $5 \times 10^{-5}$  torr in all cases

Emission Current = 28mA

Scan Voltage = maximum value of scan voltage before onset of rapid current drop

Ion Current = ion current hitting 0.2cm<sup>2</sup> detector + secondary emitted electrons

cm<sup>2</sup> and was only about 1 inch from the end of the ion gun, it measured approximately 5 $\mu$ A, about 43% higher than the current through the detector on the sample holder. Apparently, less than 70% of the ions leaving the gun were hitting the sample area when the beam was not rastered. This fraction dropped to less than 62% when the beam was rastered with a 500 V scan voltage.

The above performance was assumed to be the result of poor focusing of the beam. Since the beam was supposed to focus to a spot approximately 2.5 mm in diameter, much more than 70% of the total ion current should have hit the 5 mm diameter detector. The cause of this apparent focusing problem was not determined. One possible cause is that the clearance between the gun and the sample was 25% less than the minimum recommended by the manufacturer. This possibility was not explored because of the difficulty in moving either the sample position or the gun.

Measured etch depths and calculated etch rates for five samples are shown in Table III. The depth measurements listed were taken on a Sloan Dektak surface profile measuring system. At these very shallow etch depths, the Dektak seemed rather unreliable. Repeated surface contour measurements along the same line on a sample indicated variations in crater depth at a given point of as much as 60%. The etch depths listed in Table III are averages

Table III  
Measured Etch Depths for Selected Samples

Sample #	Beam Energy (eV)	Etch Time (Min)	Measured Etch Depth (Å)	Calculated Etch Rate (Å/min)
2	1000	120	5150	43
3	500	120	2933	24
4	500	120	1000	8.3
5	500	240	1839	7.7
6	500	338	1650	4.9

\*Ion beam not rastered on samples 2 or 3

based upon multiple surface contour scans across different parts of the samples. The etch rates listed are also averages based upon the assumption that the etch rate was a constant for each etch during the entire etch cycle.

The etch rates of samples 2 and 3 reflect the expected dependence on beam energy. A comparison of the etch rate for sample 3 with that of samples 4 and 5, illustrates the effect of current density on etch rate. With samples 4 and 5, the ion beam was rastered in an effort to obtain a more uniform etch depth across the sample. The rastering did result in a noticeably more uniform etch of the sample, but also caused a dramatic reduction in etch rate. The etch rate for sample 6 was expected to be about the same as for samples 4 and 5. The near 40% reduction in the observed etch rate for sample 6 was probably the result of a change in ion beam position. The beam position had been intentionally adjusted prior to the etch of sample 6. This adjustment was intended to improve etch depth uniformity across the sample surface but apparently had an adverse effect on the etch rate.

At this point, it is worth mentioning the time required to obtain depth-resolved luminescence data by the methods used in this study. One cycle of etching and luminescence measurement normally took approximately 2-1/2 hours. This time included 30 minutes of etching

and approximately 40 minutes for luminescence measurements with two excitation sources. The rest of the time was required for preparations such as sample temperature changes, filling the chamber with argon and pumping it out, waiting for the ion beam current to stabilize, measuring electron beam currents, and adjusting the optics. As a result, no more than about four etch cycles could be completed per day. Furthermore, changing the sample always took at least one half day because of the pump down time required for the vacuum chamber.

#### Luminescence in Virgin GaAs

Initial luminescence measurements were made on virgin samples. All virgin samples had essentially the same spectrum. Luminescence from a typical virgin sample is shown in Figures 9 and 10. Figure 9 shows photoluminescence and two different cathodoluminescence spectra from sample 4. Figure 10 shows the depth resolved cathodoluminescence from the same sample.

The main luminescence peak in all virgin samples appeared to be two unresolved lines that peaked at 1.494 eV and 1.491 to 1.490 eV. Most spectra also showed evidence of a third line on the low energy side of this main peak but it was completely unresolved in all spectra. In addition to this main peak, nearly all spectra from virgin

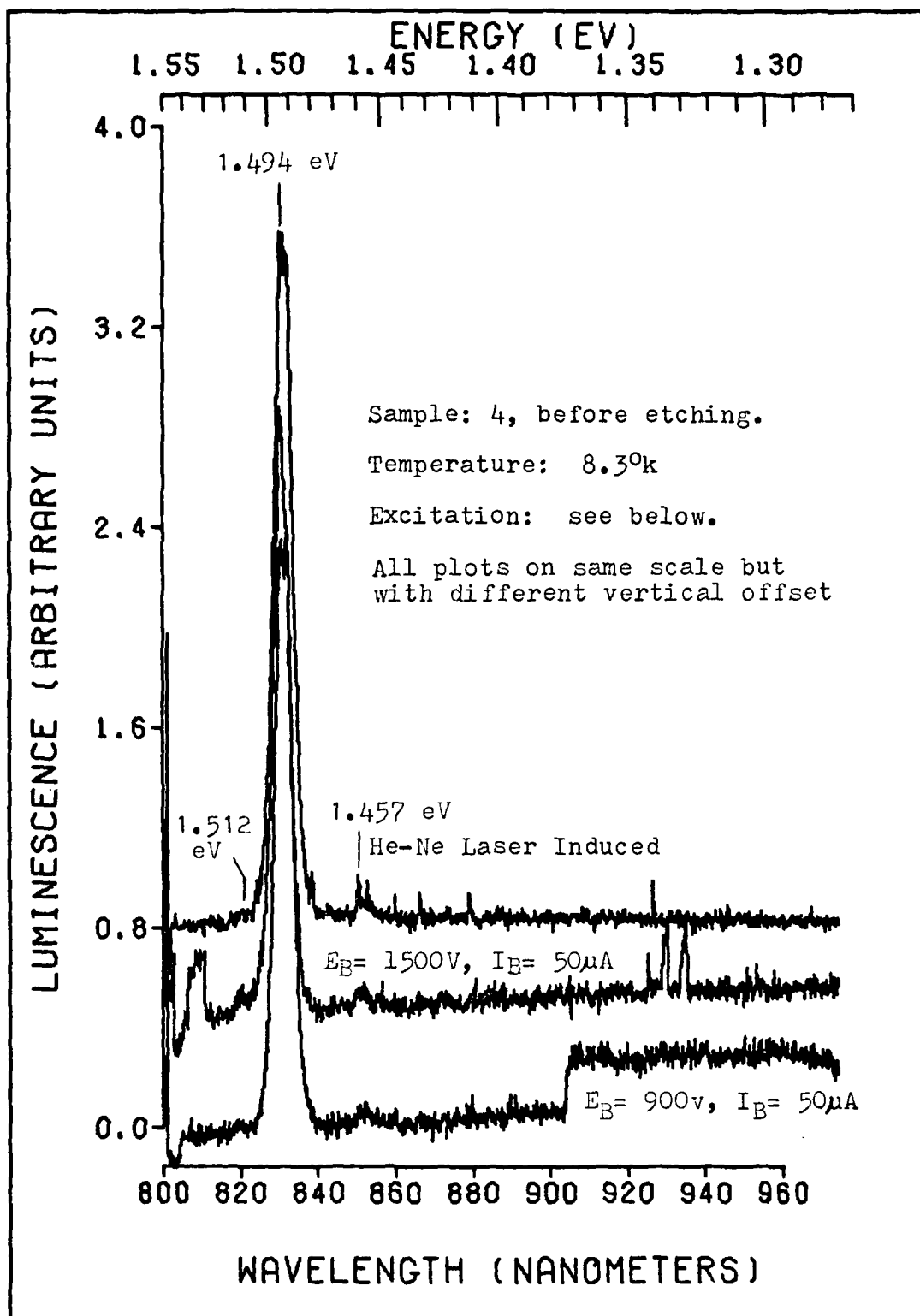


Fig. 9. Luminescence From Surface of Sample 4, various Excitation Sources.

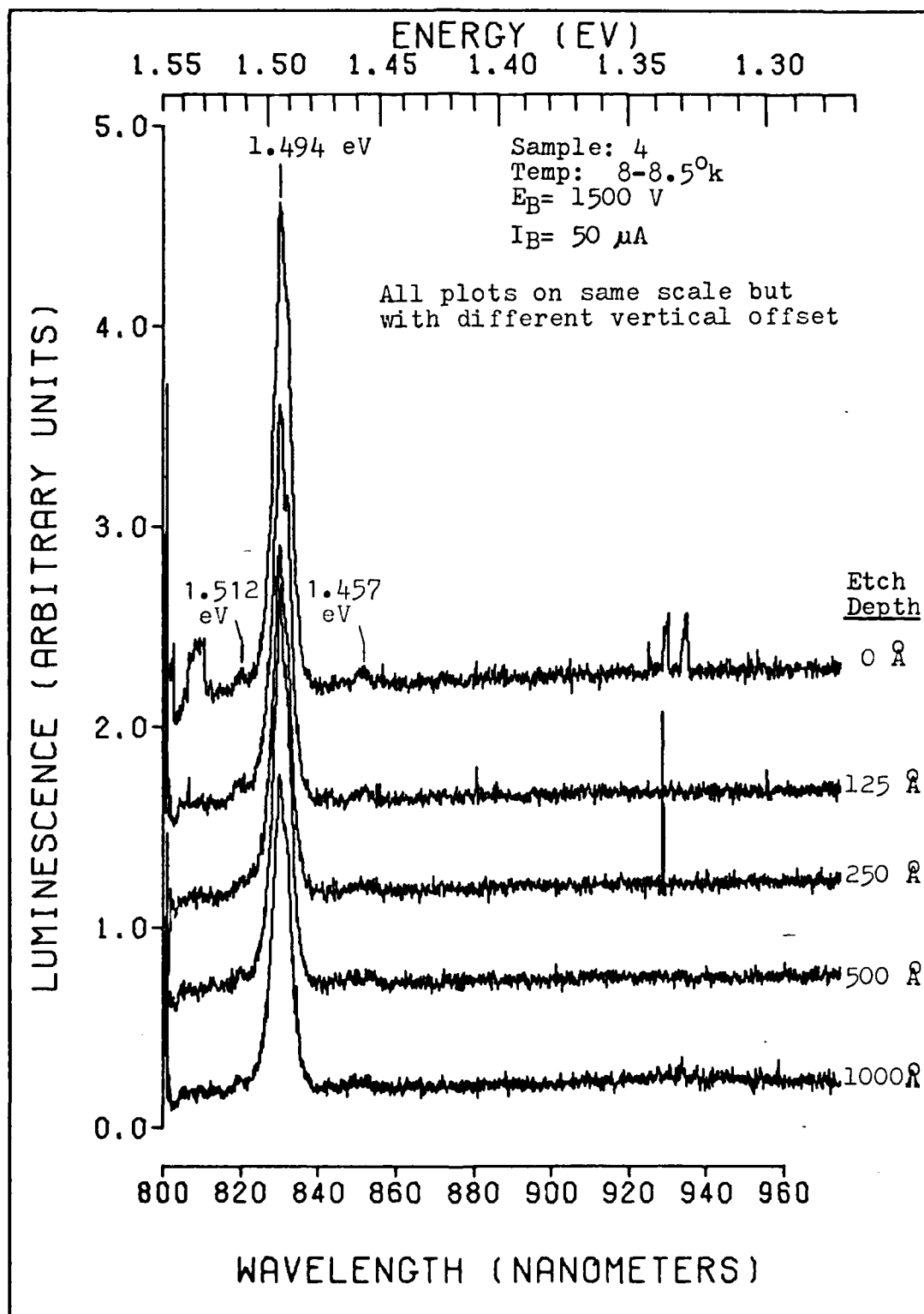


Fig. 10. Cathodoluminescence From Sample 4 at Various Etch Depths.

material showed two very weak peaks. One just below band gap at 1.512 to 1.514 eV, and another approximately 35 to 36 meV below the main peak at 1.456 to 1.458 eV. Both of these weak emission peaks appeared to be composed of two or three lines but again, they were completely unresolved.

Spark source spectrographic analysis was performed on samples from the same batch as those used in this study. The major contaminants were found to be silicon and carbon. Therefore, the spectra from these samples should correspond to published data on the luminescence of GaAs:Si and GaAs:C.

The weak peak at 1.512-1.514 eV is very probably due to bound exciton annihilation. Three bound exciton lines have been reported for GaAs:Si in this energy range (Ref. 28:342). The main peak, with lines at 1.494 eV and 1.490 eV, is believed to be the double peak commonly observed in carbon doped GaAs. This peak is the result free electrons recombining with holes bound to carbon acceptors. The weak peak at 1.456 to 1.458 eV is believed to be composed of phonon replicas of the lines in the main peak. This is believed to be the case because the energy difference between the two peaks (35 meV) is very close to the reported longitudinal optical phonon energy in GaAs (36 meV). These three luminescence peaks are present in most of the data presented here and will

be referred to throughout the rest of this discussion as the exciton peak (1.512-1.514 eV), the acceptor peak (1.490-1.494 eV), and the phonon peak (1.456-1.458 eV).

The important result shown in Figure 9 is that the virgin samples produced virtually the same luminescence spectra when excited by the He-Ne laser as when excited by either the 900 V or 1500 V electron beam. The significance of the data shown in Figure 10 is that, in virgin material, the general shape of the spectrum was essentially unaffected by ion etching to depths up to 1000 Å. There was some decreases in the signal strength due to the surface damage caused by ion etching. As a result, the exciton and phonon peaks were nearly lost in the noise, but there were no noticeable shifts in the peak energies or any gross changes in the spectra. This result was expected in the homogeneous, virgin material.

#### Luminescence in Ion Implanted, Annealed GaAs

The depth-resolved photoluminescence from sample 6 is presented in Figure 11. Sample 6 had been implanted with  $10^{14}$ , 120 keV silicon ions per  $\text{cm}^2$  and annealed for 15 minutes at 900° C. Several interesting observations can be made from the data in this figure.

The intensity of the acceptor peak from the surface of sample 6 was 20 to 100 times that of a typical virgin

sample. This result is attributed to the annealing which removes structural defects from the lattice, thereby improving surface quality and luminescence efficiency.

Another interesting feature is the increase in the relative intensity of the exciton peak and the slight increase in the energy of this peak. The peak is at 1.515 eV at the surface of sample 6. This is very close to the expected energy of a donor level to conduction band (bound electron-free hole) transition and it may be that the increased relative intensity of this peak results in part from the added silicon atoms that enter the lattice as donors.

Ion etching of sample 6 resulted in a very dramatic reduction in the intensity of the luminescence. After etching 500 Å, the peak intensity was reduced by approximately 93% while with sample 4, a similar etch resulted in a peak intensity reduction of only about 30%. This data is a little misleading because the reduction in intensity for sample 4 was much less than average. Most virgin samples experienced a reduction in luminescence intensity of about 80% after etching. The differences may simply be the result of differences in initial surface quality. If all the samples received about the same degree of surface damage from ion etching, the damage would be more apparent in the samples with the best initial surface quality.

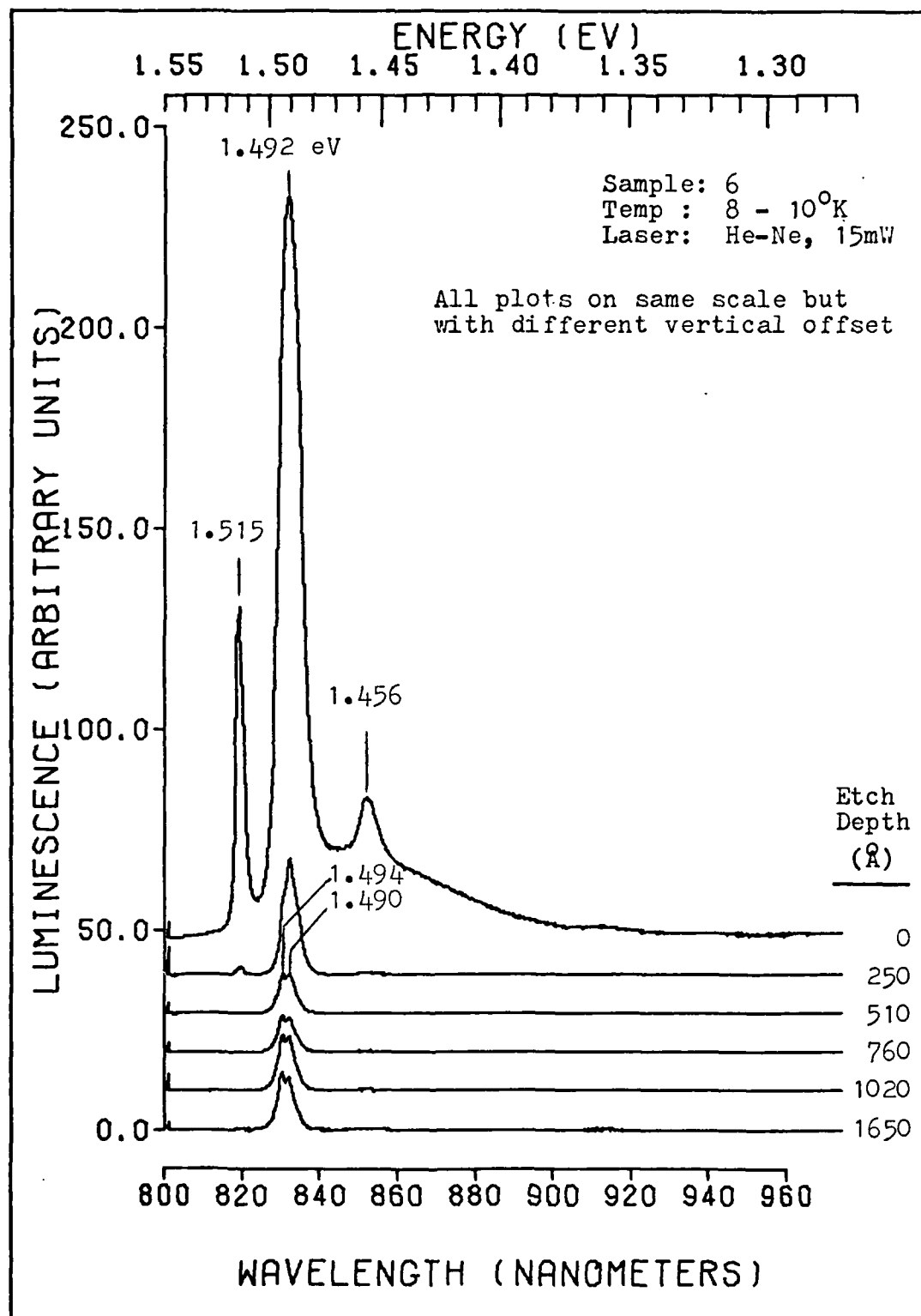


Fig. 11. Photoluminescence of Sample 6 at Various Etch Depths.

The only other obvious result shown in figure 11 is that the resolution of the acceptor peak improved after four etch cycles. This effect is not understood at this time.

In contrast to the luminescence from virgin GaAs, the cathodoluminescence of sample 6, shown in Figures 12 and 13, was very different from the photoluminescence of the same sample. The difference are believed to result from the order of magnitude difference in the penetration depth of the two excitation sources. The He-Ne laser beam penetrated approximately  $2700 \text{ \AA}$  and therefore, sampled a surface layer that was roughly as thick as the silicon implant layer while the 900 eV electron beam sampled a layer only about  $200 \text{ \AA}$  thick. As a result, the cathodoluminescence appeared to be much more sensitive to variations in impurity concentration and implantation-induced lattice damage than photoluminescence.

The data presented in figure 12 is a direct comparison of the photoluminescence and cathodoluminescence from the unetched surface of sample 6. It is obvious that the luminescence from the surface of sample 6 was dominated by a radiative complex which produced a broad band centered near 1.439 eV with a full width at half maximum of approximately 80 meV. This luminescence is believed to result

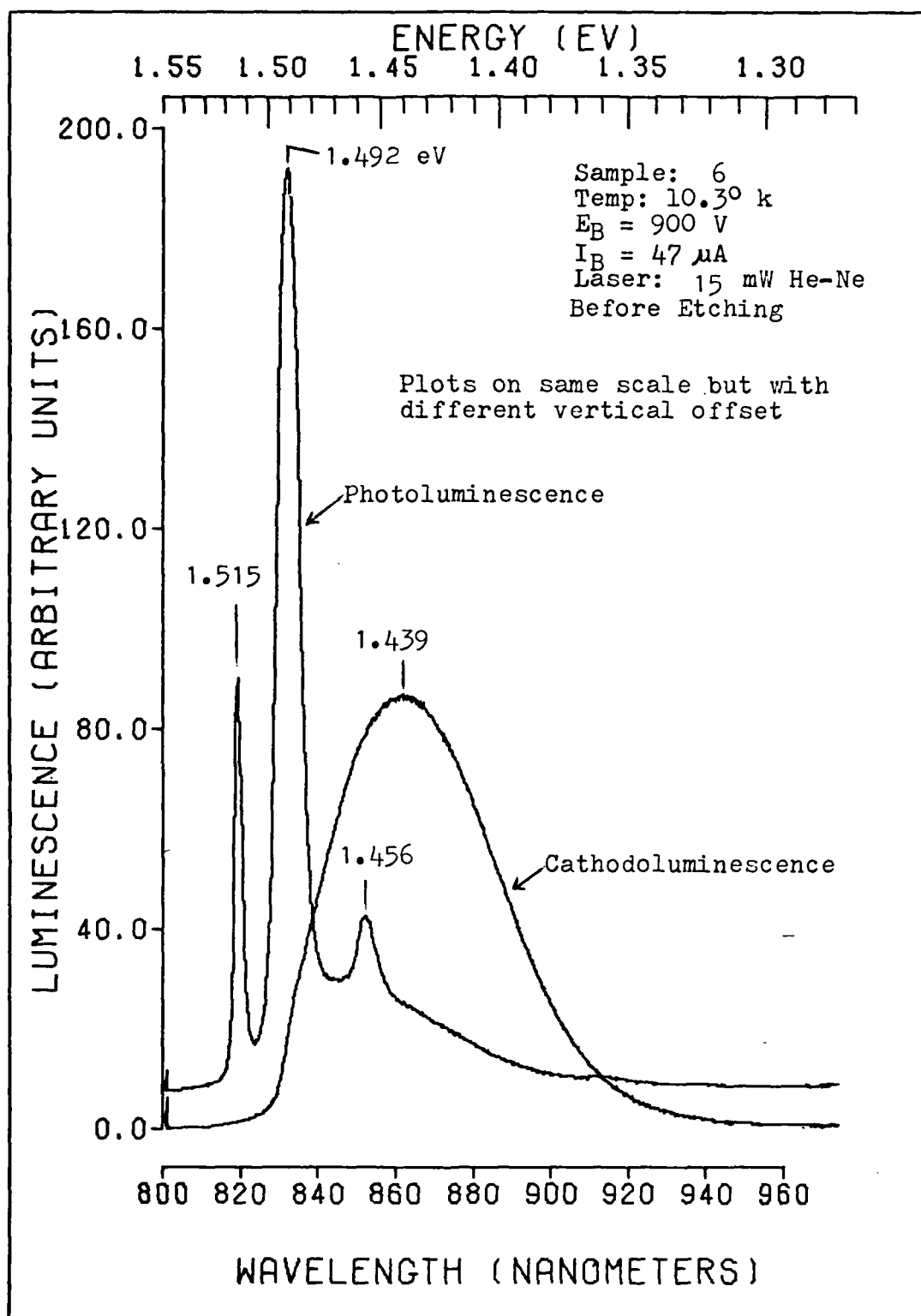


Fig. 12. Photo- and Cathodoluminescence From Surface of Sample 6.

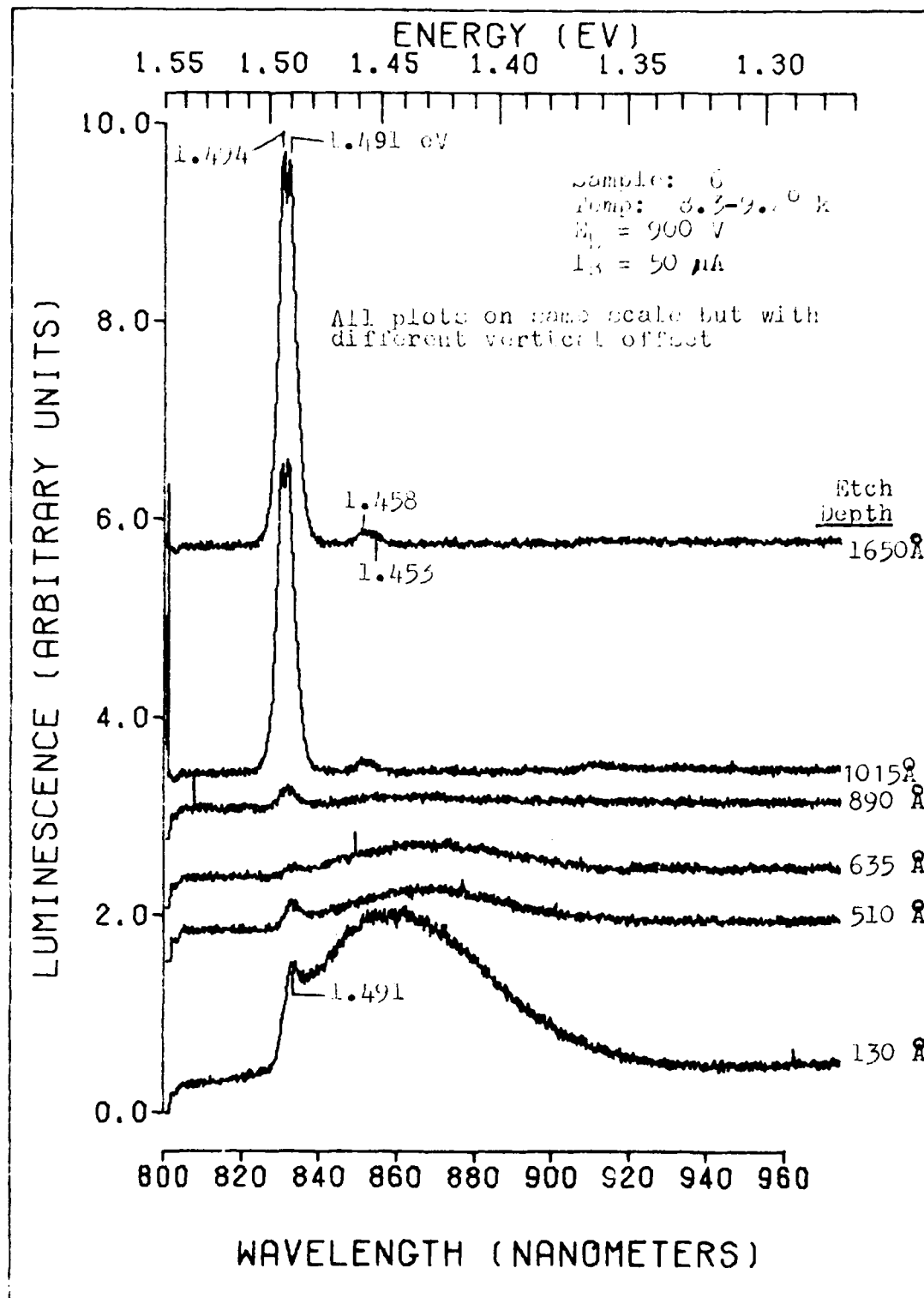


Fig. 13. Cathodoluminescence of Sample 6 at Various Etch Depths.

from a  $V_{As} - Si_{As}$  center produced by the combination of silicon implantation and annealing.

The cathodoluminescence of sample 6 at various etch depths is shown in Figure 13. It would be a mistake to try and draw any general conclusions based on the data from one sample but some observations are warranted. First, it appears that cathodoluminescence with low energy electrons may be a more sensitive analysis technique than He-Ne induced photoluminescence. Second, the acceptor peak re-appeared in the spectrum after the first etch of the sample. This would seem to indicate that the  $V_{As} - Si_{As}$  complex is most dominant only in a very thin layer near the surface. Between 500 and 800 Å the luminescence is almost completely quenched suggesting the possibility of residual implantation damage not removed by annealing. Beyond 1000 Å, the spectrum returned to nearly the same spectrum seen in virgin material. The exciton peak is still missing beyond 1000 Å but it was always the weakest part of the spectrum in damaged material. A weak peak at 1.364 eV was present after 1015 Å of etching but went away after the next etch. This peak has been attributed by others to Ga vacancies in GaAs and so its appearance was not surprising.

The luminescence is dominated by the acceptor peak and the 1.44 eV peak is gone after an etch of  $1015 \text{ \AA}$ . This is the depth at which the concentration of implanted silicon should be reaching a maximum. Therefore, the presence of the 1.44 eV peak does not correlate well with the predicted silicon concentration profile. It may be that the 1.44 eV peak is more closely associated with residual lattice damage than with silicon concentration.

#### Luminescence of Annealed GaAs

In an effort to determine if the 1.44 eV peak, observed in sample 6, was due in some way to the annealing process, the cathodoluminescence of sample 8 was measured. Sample 8 was an unimplanted sample that was subjected to the same annealing process as sample 6. The cathodoluminescence of sample 8 is shown in Figure 14. The only obvious results of the annealing were an overall increase in the luminescence intensity, as compared to virgin samples, and an increase in the relative intensity of the exciton peak. The annealing process alone was not responsible for the creation of the complex center that produced the 1.44 eV radiation.

#### Luminescence of Implanted, Unannealed GaAs

It was also of interest to learn whether or not implantation of silicon without annealing would give rise

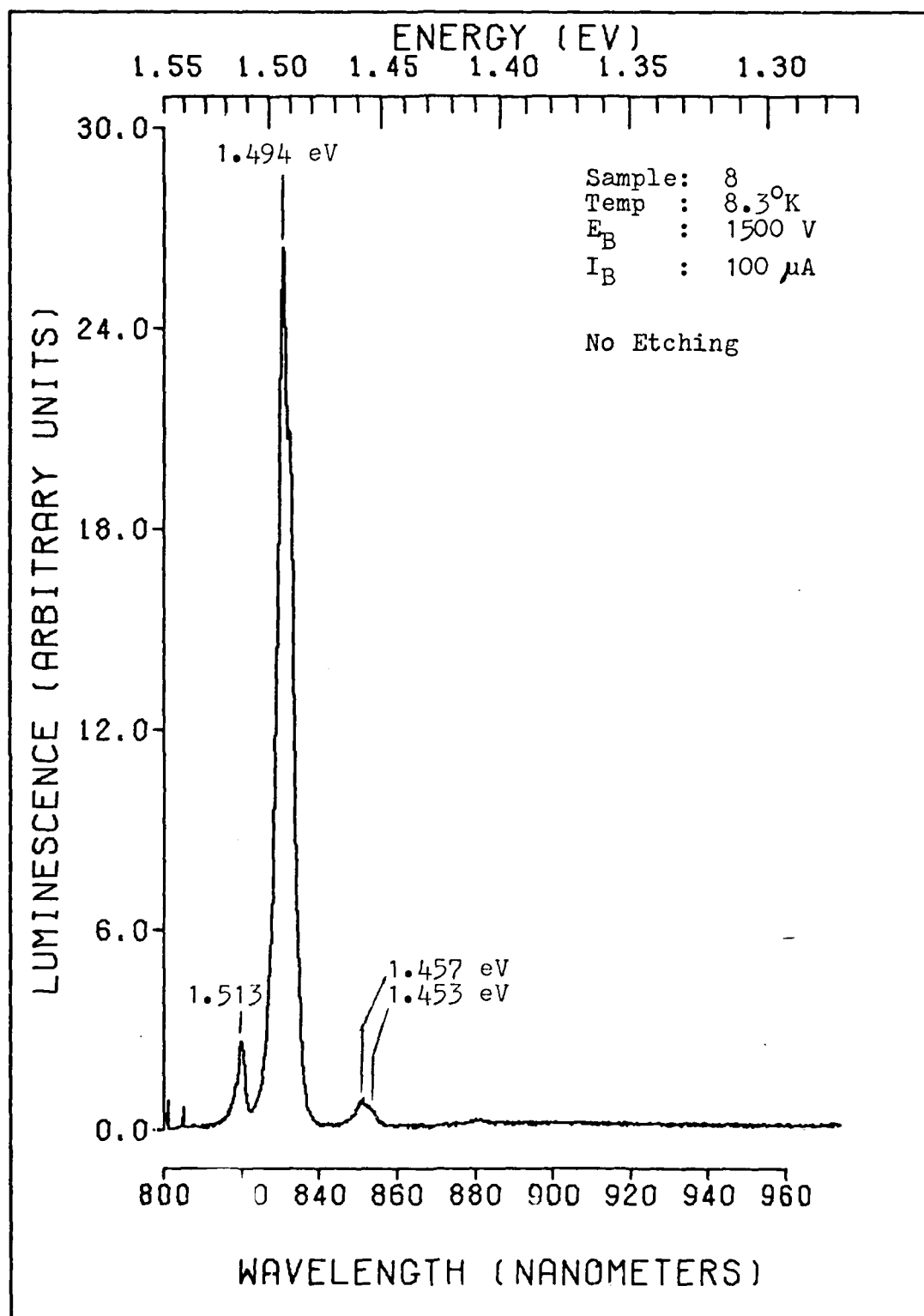


Fig. 14. Cathodoluminescence of Surface of Sample 8.

to the 1.44 eV peak. This peak was not expected in an unannealed sample because without annealing, the implanted ions are not activated and, therefore, should not affect the luminescence of the crystal. The data presented in figure 15 shows this to be the case.

Sample 7 was implanted with  $10^{14}$ , 120 keV silicon ions per  $\text{cm}^2$  just as sample 6 was, but sample 7 was not annealed. The data in figure 15 shows that the surface of the sample was so heavily damaged that all luminescence from the surface was quenched. The acceptor peak began to appear after about 760 Å had been etched away, and after 1520 Å were etched away, the acceptor peak and the phonon replica were present. The most interesting result from this depth-resolved luminescence is that the etch depth at which the luminescence appeared is roughly the same as the depth at which the normal, virgin GaAs spectrum appeared in sample 6. This is interesting because it suggests, as stated above, that the changes observed in the cathodoluminescence may be more closely related to lattice defect concentration than to impurity concentration.

The results presented in this section and the preceding one have not identified clearly the source of

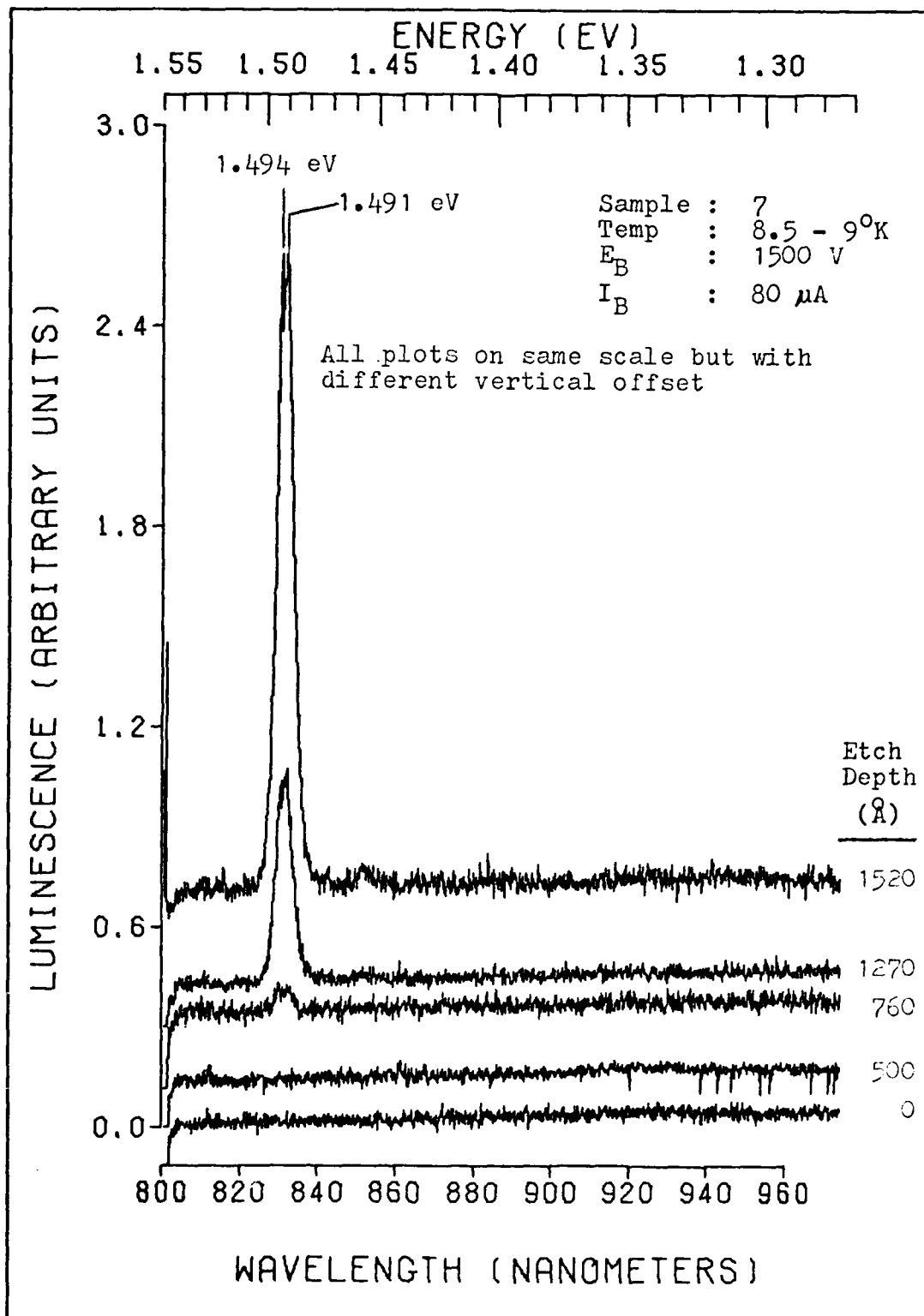


Fig. 15. Cathodoluminescence of Sample 7 at Various Etch Depths.

the 1.44 eV luminescence band. The results, however, do not contradict the theory that this band is the result of a complex center of the form  $V_{As} - Si_{As}$ . For this complex to exist, significant amounts of silicon must be present in the lattice, it must be activated by annealing, and a significant density of arsenic vacancies must also exist. These three conditions will be met in a sample that has been implanted with silicon and annealed as was the case for sample 6.

#### Luminescence in Heavily Implanted GaAs

One final sample was examined during this project. This sample, sample 9, was implanted with  $10^{15}$ , 120 keV silicon ions per  $cm^2$  and annealed at  $900^\circ C$  for 15 minutes. The sample was expected to have the same sort of luminescence spectra as observed from sample 6. The reason for looking at another such sample was to determine the sensitivity of the peak energy of the 1.44 eV peak to temperature and excitation intensity.

A direct comparison of the photoluminescence from the unetched surfaces of samples 6 and 9 is presented in figure 16. Two very interesting observations can be drawn from this figure. First, the peak intensities of the two spectra are nearly equal (approximately 175,000 counts/sec were registered by the MCA). The importance of this

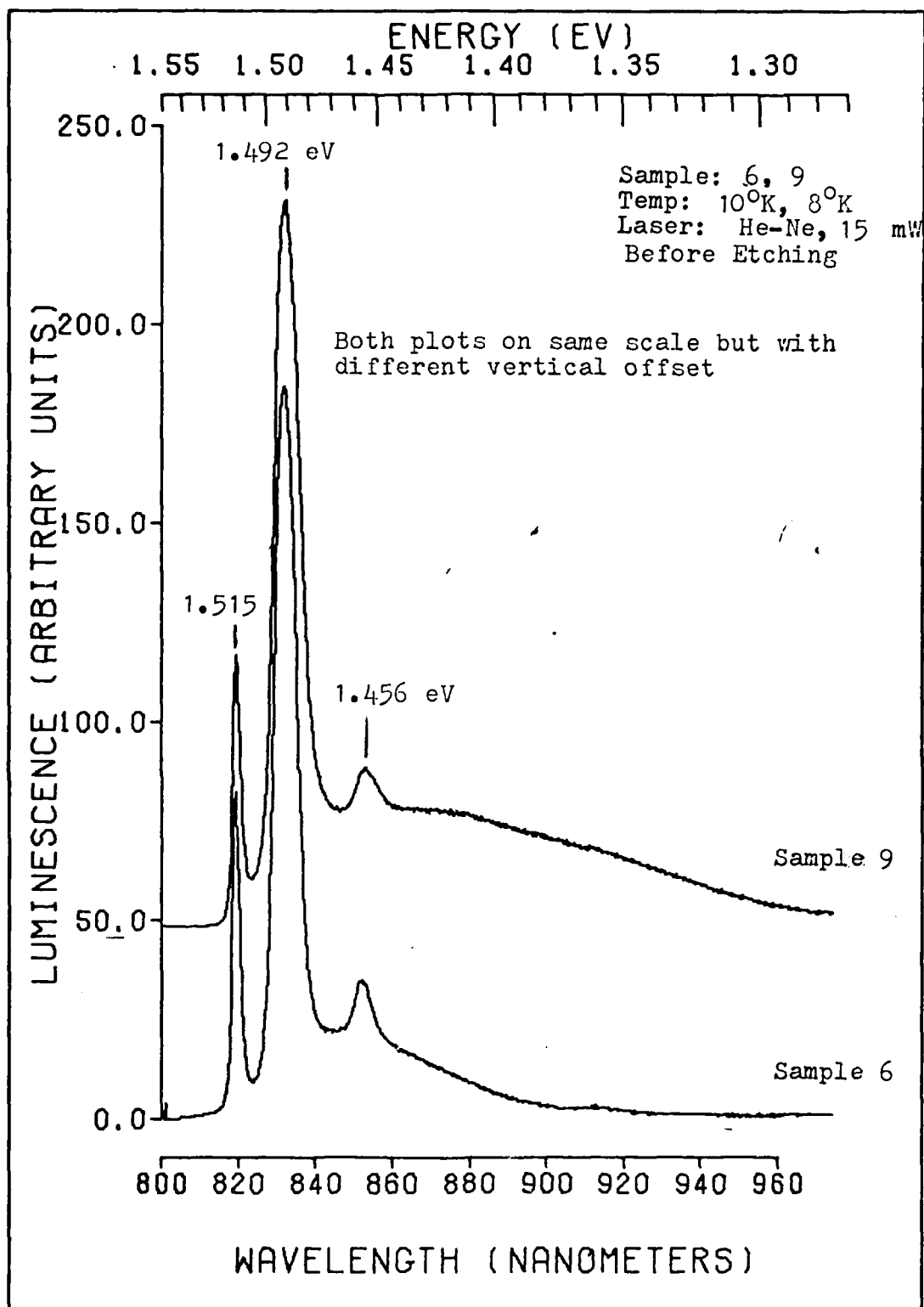


Figure 16. Photoluminescence From Surface of Samples 6 and 9.

point will become clear in the discussion of cathodoluminescence which follows later. Second, the background luminescence which appeared in both spectra was slightly more intense in sample 9 and extended to lower energies. The increased intensity of the background could be explained in the light of the higher silicon concentration in sample 9, but no explanation was found for its extension to lower energies.

The cathodoluminescence data from the unetched surfaces of sample 6 and 9 is compared in figure 17. Here, the differences are much more extreme. First of all, the intensity of the cathodoluminescence of sample 9 is nearly a factor of 40 lower than for sample 6. As pointed out earlier, the photoluminescence intensities for the two samples were nearly equal. This would seem to indicate that in a thin layer near the surface of sample 9 there was a higher concentration of non-radiative centers than in the corresponding layer of sample 6. This reduction in intensity is probably the result of increased damage caused by the higher ion dose in sample 9.

The other obvious difference in the two spectra presented in figure 17 is the shift in the peak energy. The cathodoluminescence spectrum from sample 6 had a peak intensity at 1.449 eV while the peak from sample 9 occurred at 1.355 eV. The reason for this shift is not

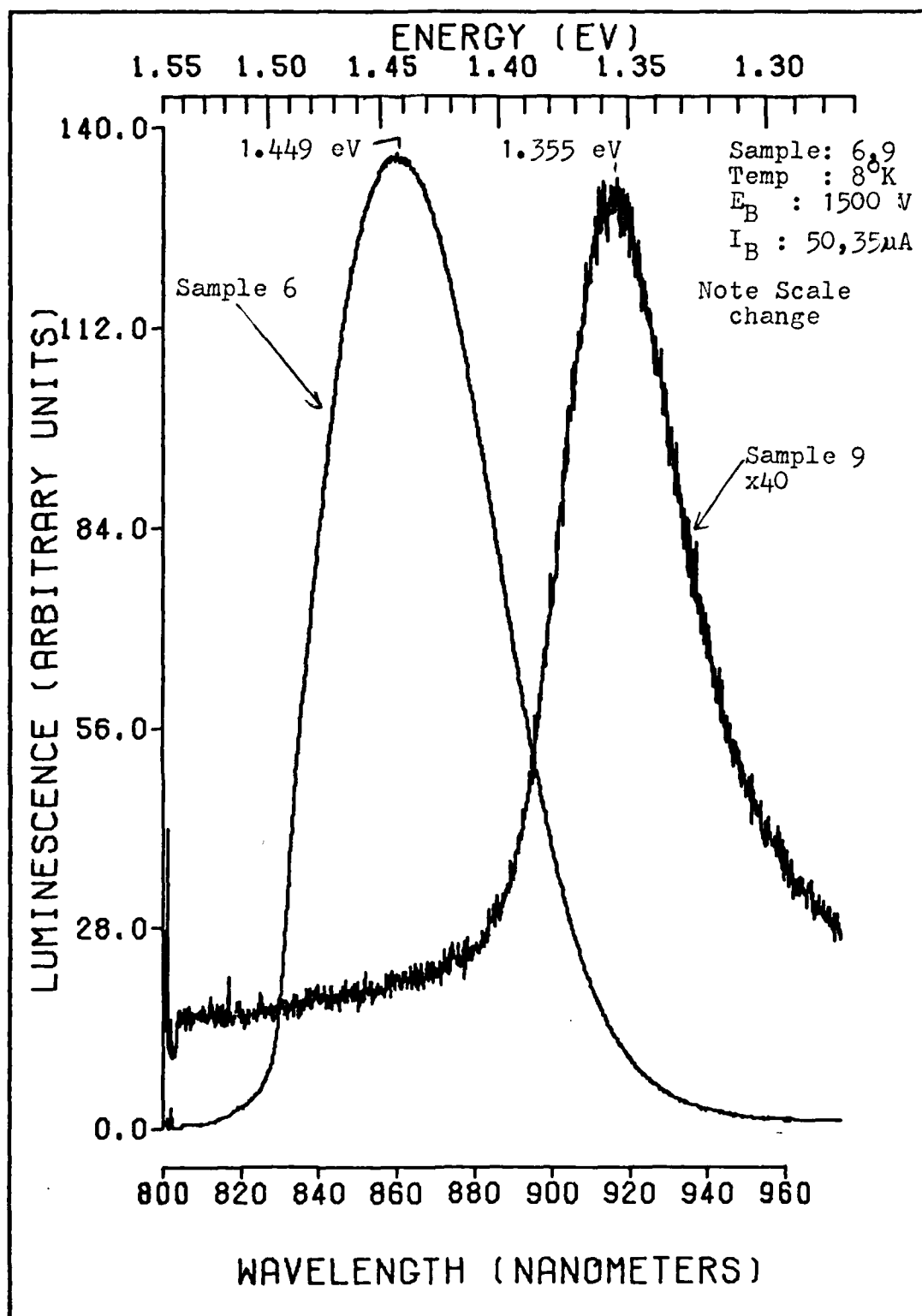


Fig. 17. Cathodoluminescence from Surface of Samples 6 and 9.

known at this time but a similar peak in the vicinity of 1.36 eV has been observed by many experimenters (Ref. 2, 3, and 15) in GaAs:Si and attributed to a complex of silicon related acceptors and arsenic vacancies ( $V_{As} - Si_{As}$ ). This is the same complex to which the 1.44 eV peak has been attributed.

The excitation intensity dependence and temperature dependence of the luminescence peak observed in sample 9 is shown in figures 18 and 19 respectively. As reported by others (Ref. 2 and 23), reductions in excitation intensity resulted in a shift of the peak to lower energy. A similar reduction in peak energy resulted from an increase in sample temperature. This phenomenon has also been reported by others (Ref. 8, 11, 12, and 23) in GaAs:Si.

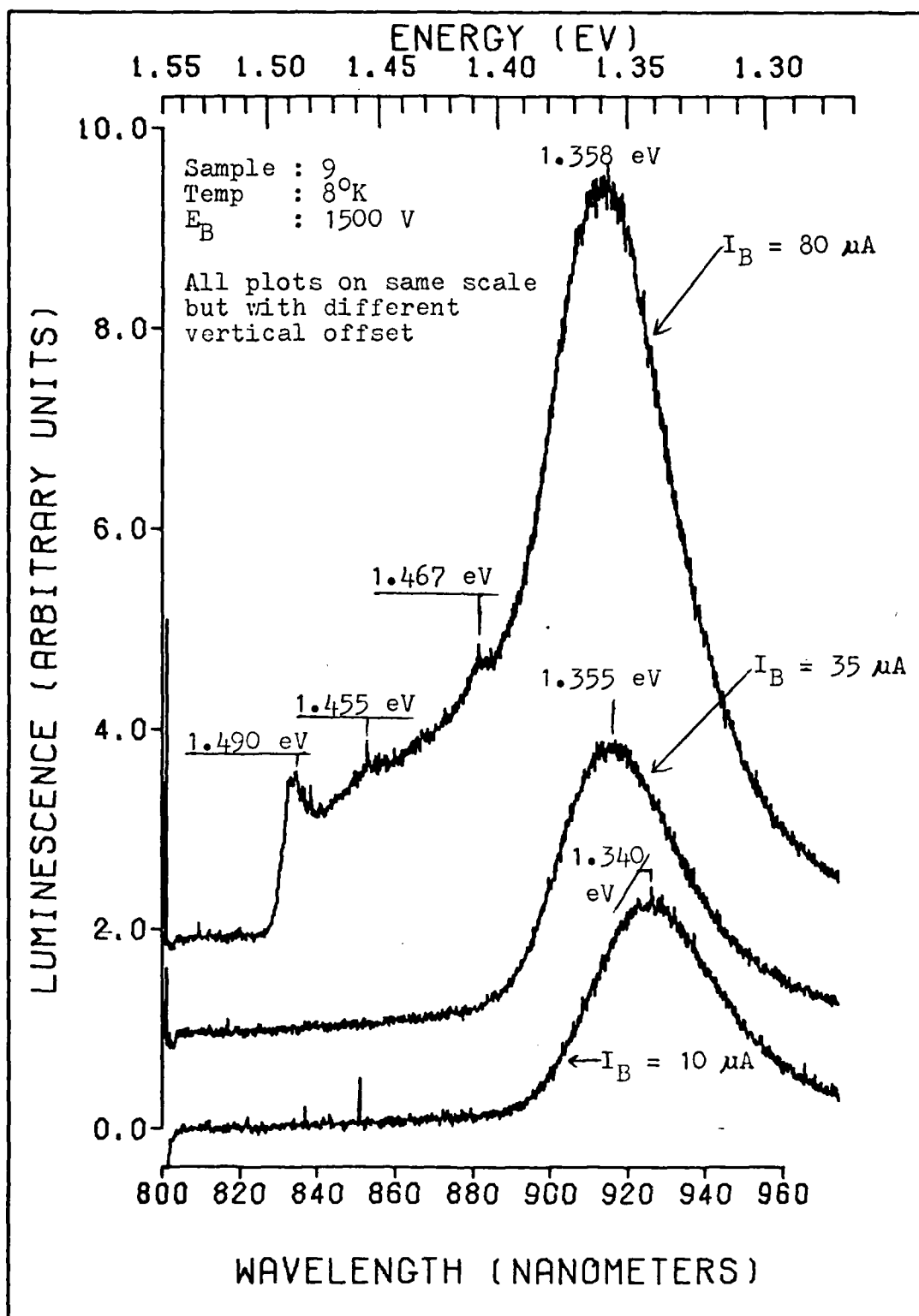


Fig. 18 . Cathodoluminescence of Sample 9 at Various Beam Currents.

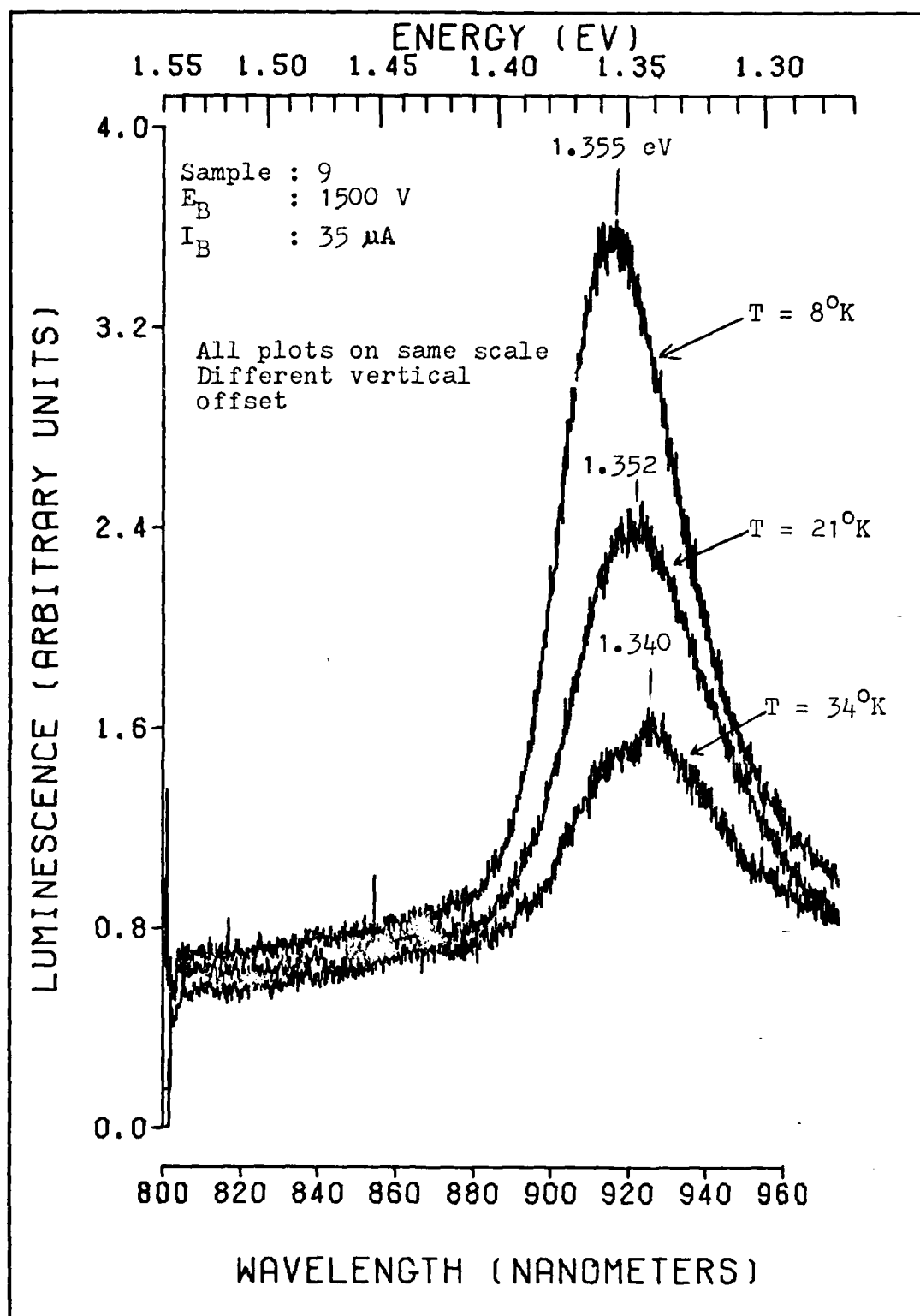


Fig. 19. Cathodoluminescence of Sample 9 at Various Temperatures.

## VI. Conclusions and Recommendations

### Conclusions

In this thesis, the depth-resolved cathodoluminescence and photoluminescence of virgin and silicon implanted GaAs were studied. Based upon the results presented in the previous chapter, the following conclusions have been reached:

1. Luminescence induced by low-energy electron bombardment is extremely sensitive to lattice damage in GaAs.
2. Depth-resolved cathodoluminescence using ion etching is effective in detecting lattice damage in annealed and unannealed, silicon implanted GaAs.
3. Ion etching with 500 eV Ar ions reduces the peak luminescence intensity by 60 to 80% in virgin GaAs and up to 93% in annealed GaAs.
4. Surface damage caused by ion etching complicates the analysis of depth-resolved luminescence data obtained by the method used in this thesis.
5. The process used in this thesis for obtaining depth-resolved luminescence data is very time consuming.

6. Implantation of 120 keV Si into GaAs followed by annealing at 900° C produces silicon-acceptor-related radiative complexes that luminesce in a broad band centered near 1.44 eV, when the Si dose is  $10^{14}$  ions/cm<sup>2</sup>, and 1.35 eV, when the Si dose is  $10^{15}$  ions/cm<sup>2</sup>. This complex was confined to a surface layer 500 to 1000 Å thick.

## Recommendations

The following recommendations are made concerning further studies and use of the system assembled during this study:

1. In future luminescence studies on ion implanted GaAs, use excitation sources with short penetration depths such as low-energy electron beams, He-Cd lasers, or ultra-violet lamps.
2. The nature of the radiative complex attributed to the interaction of Si on As sites with As vacancies should be investigated further. Its dependence on Si concentration, annealing temperature, and annealing time should be determined. Electrical measurements should be performed to determine how this complex affects the electrical properties of the semiconductor.
3. In future depth-resolved luminescence studies, use chemical etching to avoid the problems associated with ion etching and to avoid the necessity of working in ultra-high vacuum.
4. If the ion bombardment gun is used again, modify the system to move it farther back from the sample.

5. Use an X-Y plotter in conjunction with the Hewlett-Packard MCA to get a picture of each spectrum for use in comparative analysis.
6. Find an alternate way of obtaining high quality plots of the data. The routine of storing data on paper tape, transferring it to cards, and running a Calcomp program is just too slow.

AD-A111 139

AIR FORCE INST OF TECH WRIGHT-PATTERSON AFB OH SCHOOL--ETC F/8 28/2  
DEPTH-RESOLVED LUMINESCENCE OF GALLIUM ARSENIDE USING ION ETCHING--ETC(U)  
DEC 81 M Y MAGLIN  
AFIT/SEP/PH/SID-6

UNCLASSIFIED

NL

2012  
RE  
2011-09



END

DATE

FILMED

4-82

DTIC

### Bibliography

1. Arnaudov, B.G., et al. "Luminescence of Silicon - Doped Epitaxial Gallium Arsenide," Soviet Physics - Semiconductors, 11 (2): 134-135 (February 1977).
2. Birey, Hulya and James Sites. "Radiative Transitions Induced in Gallium Arsenide by Modest Heat Treatment," Journal of Applied Physics, 51 (1): 619-624 (January 1980).
3. Birey, Hulya, et al. "Photoluminescence of Gallium Arsenide Encapsulated with Aluminum Nitride and Silicon Nitride," Applied Physics Letters, 35 (8): 623-625, (October 1979)
4. Fairman, Robert D., et al. "Growth of High - Purity Semi - Insulating Bulk GaAs for Integrated - Circuit Applications," IEEE Transactions on Electron Devices, 28 (2): 135-149 (February 1981).
5. Feldman, Charles, "Range of 1 - 10 keV Electrons in Solids," Physical Review, 117 (2): 455-459 (January 1960).
6. Gershenzon, M. in Semiconductors and Semimetals, Volume 2, page 316, edited by Rik Willardson and A.C. Beers. New York: Academic Press (1966).
7. Hobgood, H.M., et al. "High-Purity Semi-Insulating GaAs Material for Monolithic Microwave Integrated Circuits," IEEE Transactions on Electron Devices, 28 (2): 140-149 (1981).
8. Hwang, C.J. "Evidence for Luminescence Involving Arsenic Vacancy - Acceptor Centers in p - Type GaAs," Physical Review, 180 (3): 827-832 (April 1969).
9. Itoh, Tadatougu and Masami Takeuchi. "Arsenic Vacancy Formation in GaAs Annealed in Hydrogen Gas Flow," Japanese Journal of Applied Physics, 16 (2):
10. Kawabe, M., et al. "Effects of Ion Etching on the Properties of GaAs." Applied Optics, 17 (16): 2556-2561 (August 1978).
11. Kressel, H., et al. "Luminescence in Silicon - Doped GaAs Grown by Liquid - Phase Epitaxy," Journal of Applied Physics, 39 (4): 2006-2011 (March 1968).

12. Kressel, H. and H. Nelson. "Electrical and Optical Properties of n - Type Si - Compensated GaAs Prepared by Liquid - Phase Epitaxy," Journal of Applied Physics, 40 (9): 3720-3725 (August 1969).
13. Kroger, F.A. The Chemistry of Imperfect Crystals. Amsterdam: North - Holland Publishing Company 1964.
14. Kung, J.K. and W.G. Spitzer. "Si - Defect Concentrations in Heavily Si - Doped GaAs: Changes Induced by Annealing," Journal of Applied Physics, 45 (10): 4477-4486 (October 1974).
15. Lum, W.Y. and H.H. Wieder. "Photoluminescence of Thermally Treated n - Type Si - Doped GaAs," Journal of Applied Physics, 49 (12): 6187-6188 (December 1978).
16. Lusk, Ronald L. Cathodoluminescence on the Effects of Te Implantation and Laser Annealing in Gallium Arsenide. Unpublished thesis. Wright-Patterson Air Force Base, Ohio: Air Force Institute of Technology, December 1978.
17. Martinelli, R.U. and CC. Wang. "Electron-beam Penetration in GaAs," Journal of Applied Physics, 44: 3350-3351 (July 1973).
18. McGuire, G.E. "Effects of Ion Sputtering on Semiconductor Surface," Surface Science, 76: 130-147 (1978).
19. Namba, S., et al. "Photoluminescence Measurement of Ion - Etched GaAs Surface," Journal of Vacuum Science and Technology, 12 (6): 1348-1351
20. Pankove, L.I. "Cathodoluminescence of n - Type GaAs," Journal of Applied Physics, 39 (12): 5368-5371 (November 1968).
21. Pierce, B.J. Luminescence and Hall Effects of Ion Implanted Layers in ZnO, Unpublished Dissertation, Wright-Patterson Air Force Base, Ohio: Air Force Institute of Technology (1974).
22. Queisser, H.J. "Photoluminescence of Silicon - Compensated Gallium Arsenide," Journal of Applied Physics, 37: 2909-2910 (1976).

23. Redfield, D., et al. "Luminescent Properties of Energy - Band - Tail States in GaAs:Si," Physical Review B, 2 (6): 1830-1839 (September 1970).
24. Rosenstein, M., et al. "Electron Depth Dose in Polystyrene," Journal of Applied Physics, 43: 3197 (July 1972).
25. Rossi, J.A., et al. "Laser Transitions in p - Type GaAs:Si," Journal of Applied Physics, 40 (8): 3289-3293 (July 1969).
26. Sturge, M.D. "Optical Absorption of Gallium Arsenide Between 0.6 and 2.75 eV," Physical Review, 127 (3): 768-773 (August 1962).
27. Williams, E.W. and H.B. Bebb. "Photoluminescence in Lightly Doped Epitaxial GaAs:Cd and GaAs:Si," Journal of Physics and Chemistry of Solids, 30: 1289-1293 (September 1968).
28. Williams, E.W. and H.B. Bebb. "Photoluminescence II: Gallium Arsenide," Semiconductors and Semimetals, Volume 8, edited by R.K. Willardson and A.C. Beer New York: Academic Press, 1972.
29. Williams, E.W. and C.T. Elliott. "Luminescence Studies of a New Line Associated with Germanium in GaAs," British Journal of Applied Physics, 2 (2): 1657-1665 (1969).

Vita

1

Myron Travis Maclin was born on 8 April 1954, in Malden, Missouri, the son of the John Travis and Della Marilyn Maclin. He attended Twin Rivers High School in Broseley, Missouri. Upon graduation in 1972, he accepted a four-year, AFROTC college scholarship and entered South East Missouri State University in Cape Girardeau, Missouri. In 1976, he graduated Magna Cum Laude with a Bachelor of Science degree in Physics and Mathematics and received a commission in the United States Air Force. He was ordered to active duty in August 1976 when he was assigned to the Air Force Rocket Propulsion Laboratory, Edwards Air Force Base, California. In June 1980, he was assigned to the Air Force Institute of Technology.

Permanent address: 405 North Miller St.  
Bernie, Missouri  
63822

Unclassified

SECURITY CLASSIFICATION OF THIS PAGE (When Data Entered)

REPORT DOCUMENTATION PAGE		READ INSTRUCTIONS BEFORE COMPLETING FORM
1. REPORT NUMBER AFIT/GEP/PH/81-6	2. GOVT ACCESSION NO. AD-A111 139	3. RECIPIENT'S CATALOG NUMBER
4. TITLE (and Subtitle) DEPTH-RESOLVED LUMINESCENCE OF GALLIUM ARSENIDE USING ION ETCHING		5. TYPE OF REPORT & PERIOD COVERED MS THESIS
		6. PERFORMING ORG. REPORT NUMBER
7. AUTHOR(s) Myron T. Maclin Capt., USAF		8. CONTRACT OR GRANT NUMBER(s)
9. PERFORMING ORGANIZATION NAME AND ADDRESS Air Force Institute of Technology (AFIT/EN) Wright-Patterson AFB, Ohio 45433		10. PROGRAM ELEMENT, PROJECT, TASK AREA & WORK UNIT NUMBERS
11. CONTROLLING OFFICE NAME AND ADDRESS		12. REPORT DATE December 1981
		13. NUMBER OF PAGES 98
14. MONITORING AGENCY NAME & ADDRESS (if different from Controlling Office)		15. SECURITY CLASS. (of this report) Unclassified
		15a. DECLASSIFICATION/DOWNGRADING SCHEDULE
16. DISTRIBUTION STATEMENT (of this Report) Approved for public release; distribution unlimited.		
17. DISTRIBUTION STATEMENT (of the abstract entered in Block 20, if different from Report)		
18. SUPPLEMENTARY NOTES Approved for public release; IAW AFR 190-17 28 JAN 1982 <i>Frederick C. Lynch</i> Frederick C. Lynch, Major, USAF Director of Public Affairs		
19. KEY WORDS (Continue on reverse side if necessary and identify by block number) Cathodoluminescence Photoluminescence Gallium Arsenide Ion Etching		
20. ABSTRACT (Continue on reverse side if necessary and identify by block number) A system was assembled for obtaining depth-resolved, low-temperature luminescence data from GaAs using ion etching. This system was tested on virgin and silicon implanted, liquid-encapsulated Czochralski (LEC) grown GaAs. It was found to be effective in detecting lattice damage in annealed and unannealed Si-implanted GaAs. Cathodoluminescence, using a low-voltage (900-1500 V), high current (50-100 $\mu$ A) (Continued)		

DD FORM 1473

JAN 73

EDITION OF 1 NOV 65 IS OBSOLETE

Unclassified

SECURITY CLASSIFICATION OF THIS PAGE (When Data Entered)

Unclassified

SECURITY CLASSIFICATION OF THIS PAGE(When Data Entered)

electron gun, was found to be extremely sensitive to surface defects. Very intense, broad ( $\sim 80$  meV) luminescence bands were observed near 1.44 eV in GaAs implanted with  $10^{14}$  Si ions/cm<sup>2</sup> and near 1.35 eV in GaAs implanted with  $10^{15}$  Si ions/cm<sup>2</sup>. The center(s) responsible for this luminescence was confined to a surface layer 500-1000 Å thick.

Unclassified

SECURITY CLASSIFICATION OF THIS PAGE(When Data Entered)

